

Convexification Numerical Method for a Coefficient Inverse Problem for the Riemannian Radiative Transfer Equation

Michael V. Klibanov^{1*}, Jingzhi Li², Loc H. Nguyen¹, Vladimir G. Romanov³ and Zhipeng Yang⁴

^{1*}Department of Mathematics and Statistics, University of North Carolina at Charlotte, Charlotte, NC, 28223, USA.

²Department of Mathematics & National Center for Applied Mathematics Shenzhen & SUSTech International Center for Mathematics, Southern University of Science and Technology, Shenzhen, 518055, P. R. China.

³Sobolev Institute of Mathematics, Novosibirsk, 630090, Russian Federation.

⁴Department of Mathematics, Southern University of Science and Technology, Shenzhen, 518055, P. R. China.

*Corresponding author(s). E-mail(s): mklibanv@uncc.edu;
Contributing authors: li.jz@sustech.edu.cn; loc.nguyen@uncc.edu;
romanov@math.nsc.ru; yangzp@sustech.edu.cn;

Abstract

The first globally convergent numerical method for a Coefficient Inverse Problem (CIP) for the Riemannian Radiative Transfer Equation (RRTE) is constructed. This is a version of the so-called “convexification” principle, which has been pursued by this research group for a number of years for some other CIPs for PDEs. Those PDEs are significantly different from RRTE. The presence of the Carleman Weight Function (CWF) in the numerical scheme is the key element of the convexification. CWF is the function, which is involved as the weight function in the Carleman estimate for the corresponding PDE operator. Convergence analysis is presented along with the results of numerical

experiments, which confirm the theory. RRTE governs the propagation of photons in the diffuse medium in the case when they propagate along geodesic lines between their collisions. Geodesic lines are generated by the spatially variable dielectric constant of the medium.

Keywords: geodesic lines, Riemannian metric, Carleman estimate, coefficient inverse problem, global convergence, convexification, numerical studies.

MSC Classification: 35R30 , 65M32

1 Introduction

This is the first publication, in which a globally convergent numerical method, the so-called convexification, is constructed for a Coefficient Inverse Problem (CIP) for the steady state so-called Riemannian Radiative Transfer Equation (RRTE). In the case of inverse problems for the steady state Radiative Transfer Equation (RTE), numerical methods were mostly developed for inverse source problems [15–17, 59], which are linear ones. On the other hand, CIPs are nonlinear. We refer to the recent publication [46] for the convexification numerical method for a CIP for RTE. The authors are unaware about other numerical methods for CIPs for RTE and RRTE.

The key element of our numerical method is the presence of a Carleman Weight Function (CWF) in a certain weighted least squares cost functional. This presence ensures the global strict convexity of that functional. This is why we call our method “convexification”. The CWF is involved as the weight function in the Carleman estimate for the corresponding PDE operator. Our convergence analysis ensures the global convergence of the gradient descent method of the minimization of that functional to the true solution of our CIP, as long as the level of the noise in the data tends to zero. In addition to a Carleman estimate, the apparatus of the Riemannian geometry is used here. Results of numerical experiments are presented, and they confirm our theory.

The conventional steady state RTE governs light propagation in the diffuse medium, such as, e.g. turbulent atmosphere and biological media [24]. Inverse problems for RTE have applications in, e.g. problems of seeing through a turbulent atmosphere and in an early medical diagnostics. In the latter case the near infrared light with a relatively small energy of photons is used, see, e.g. [3, 60]. However, it is assumed in RTE that photons propagate along straight lines between their collisions. On the other hand, since the dielectric constants in heterogeneous media, such as, e.g. ones mentioned above, vary in space, then photons actually propagate along geodesic lines between their collisions. These lines are generated by the Riemannian metric $\sqrt{\varepsilon_r(\mathbf{x})}|d\mathbf{x}|$. Here and below $\mathbf{x} = (x, y, z) \in \mathbb{R}^3$ and $\varepsilon_r(\mathbf{x})$ is the spatially distributed dielectric constant, so that $n(\mathbf{x}) = \sqrt{\varepsilon_r(\mathbf{x})}$ is the refractive index. To take this into account, the so-called Riemannian Radiative Transport Equation (RRTE) should be used.

To study our CIP, we derive first a constructive proof of an existence and uniqueness theorem for the forward problem for RRTE. An important assertion of this theorem, which is significantly used for our numerical method for the CIP, is the claim about the positivity of the solution of the forward problem. Previously this positivity was proven only for the case of RTE in [46]. From the numerical perspective, this theorem allows us to solve RRTE numerically as a linear integral equation with integrals over geodesic lines. We use this solution to computationally simulate the data for our inverse problem. Other existence and uniqueness results for the forward problems for RTE and RRTE, although without claims of the positivity of solutions, can be found in [6, 59, 60]. The form of RRTE in [6] is more general than the one of this paper.

In the past, various uniqueness and stability results for inverse problems for RTE and RRTE, including quite general forms of the later equation, were proven in, e.g. [3–6, 36, 37, 47, 51, 52, 60, 61], [56, Chapter 5]. On the other hand, we are interested in the numerical method for our CIP.

The phenomena of ill-posedness and nonlinearity of CIPs are well known and cause serious challenges for their numerical solutions. Both a powerful and popular concept of numerical methods for CIPs is based on the minimization of appropriate least squares cost functionals, see, e.g. [1, 8, 9, 14, 18, 20, 21, 23] and references cited therein. Since such a cost functional typically is non convex, then it usually suffers from the phenomenon of local minima and ravines, see, e.g. [58], i.e. the availability of a good first guess about the true solution is a necessary assumption of the convergence analysis.

Definition 1.1. *We call a numerical method for a CIP globally convergent if a theorem is proven, which claims that this method delivers at least one point in a sufficiently small neighborhood of the true solution without any advanced knowledge of this neighborhood. The size of that neighborhood should depend only on the level of noise in the data.*

The convexification concept generates globally convergent numerical methods since such a method does not rely on a good first guess about the solution. The convexification was originally proposed in purely theoretical works [34, 35]. Its active numerical studies have started in 2017 after the publication [2], which has removed some obstacles for numerical implementations. In this regard, we refer to, e.g. [7, 11, 30, 31, 40, 41, 44, 46] for some publications, which combine convergence analysis with numerical results. The book [43] summarizes results as of 2021. Note that in [31, 40], [43, Chapter 10] the convexification is verified on experimentally collected data of backscatter microwaves.

Carleman estimates were first introduced in the pioneering work of Carleman [13]. Since then they have been actively used for proofs of uniqueness and stability results for ill-posed Cauchy problems, see, e.g. books [25, 27, 48]. Carleman estimates were introduced in the field of Coefficient Inverse Problems in the publication [12] initially with the single goal of proofs of uniqueness theorems. Since then the idea of [12] became popular, see, e.g. [10, 26, 27, 32, 33, 38, 43, 64]. The convexification principle represents an

4 *Convexification method for CIP for RRTE*

extension of the idea of [12] to the topic of globally convergent numerical methods for CIPs. Those numerical methods might be generalized and employed for important applications like cloaking and quantum scattering studied in [49, 50].

All functions considered below are real valued ones. For the sake of definiteness, we work below in our theoretical derivations only with the 3d case, the 2d case is completely similar. In section 2 we pose both the forward and inverse problems for RRTE. In section 3 we formulate and prove existence and uniqueness theorem for the forward problem. In section 4 we derive a version of the convexification method for our CIP. In section 5 we formulate theorems of the convergence analysis. These theorems are proven in section 6. Section 7 is devoted to numerical studies, which confirm our theory.

2 Statements of Forward and Inverse Problems

Let numbers $A, a, b, d > 0$, where

$$0 < a < b. \quad (2.1)$$

Define the rectangular prism $\Omega \subset \mathbb{R}^3$ and parts $\partial_1\Omega, \partial_2\Omega, \partial_3\Omega$ of its boundary $\partial\Omega$ as well as the line Γ_d where the external sources are as:

$$\Omega = \{\mathbf{x} : -A < x, y < A, a < z < b\}, \quad (2.2)$$

$$\partial_1\Omega = \{\mathbf{x} : -A < x, y < A, z = a\}, \quad (2.3)$$

$$\partial_2\Omega = \{\mathbf{x} : -A < x, y < A, z = b\}, \quad (2.4)$$

$$\partial_3\Omega = \{x = \pm A, y \in (-A, A), z \in (a, b)\} \cup \quad (2.5)$$

$$\cup \{y = \pm A, x \in (-A, A), z \in (a, b)\},$$

$$\Gamma_d = \{\mathbf{x}_\alpha = (\alpha, 0, 0) : \alpha \in [-d, d]\}. \quad (2.6)$$

Hence, Γ_d is a part of the x -axis. By (2.1), (2.2) and (2.6) $\Gamma_d \cap \overline{\Omega} = \emptyset$.

Let the points of external sources $\mathbf{x}_\alpha \in \Gamma_d$. Let $\epsilon > 0$ be a sufficiently small number. To avoid dealing with singularities, we model the $\delta(\mathbf{x})$ -function as:

$$f(\mathbf{x}) = C_\epsilon \begin{cases} \exp\left(\frac{|\mathbf{x}|^2}{\epsilon^2 - |\mathbf{x}|^2}\right), & |\mathbf{x}| < \epsilon, \\ 0, & |\mathbf{x}| \geq \epsilon, \end{cases} \quad (2.7)$$

where the constant C_ϵ is such that

$$C_\epsilon \int_{|\mathbf{x}| < \epsilon} \exp\left(\frac{|\mathbf{x}|^2}{\epsilon^2 - |\mathbf{x}|^2}\right) d\mathbf{x} = 1. \quad (2.8)$$

Hence, the function $f(\mathbf{x} - \mathbf{x}_\alpha) = f(x - \alpha, y, z) \in C^\infty(\mathbb{R}^3)$ plays the role of the source function for the point source $\{\mathbf{x}_\alpha\}$. We choose ϵ so small that

$$f(\mathbf{x} - \mathbf{x}_\alpha) = 0, \quad \forall \mathbf{x} \in \overline{\Omega}, \quad \forall \mathbf{x}_\alpha \in \Gamma_d. \quad (2.9)$$

Let $\Gamma(\mathbf{x}, \mathbf{x}_0)$ be the geodesic line generated by the Riemannian metric $\sqrt{\varepsilon_r(\mathbf{x})} |d\mathbf{x}|$ and connecting the source $\mathbf{x}_0 \in \mathbb{R}^{n+1}$ with an arbitrary point $\mathbf{x} \in \mathbb{R}^{n+1}$,

$$\Gamma(\mathbf{x}, \mathbf{x}_0) = \operatorname{argmin} \left\{ \begin{array}{l} \int_{\gamma} \sqrt{\varepsilon_r(\xi(t))} dt, \text{ where } \gamma(t) : [0, 1] \rightarrow \mathbb{R}^3 \\ \text{is a smooth map with } \gamma(0) = \mathbf{x}_0, \gamma(1) = \mathbf{x}. \end{array} \right\} \quad (2.10)$$

Here $\varepsilon_r(\mathbf{x})$ is the spatially distributed dielectric constant of the medium, $1/\sqrt{\varepsilon_r(\mathbf{x})}$ is the dimensionless speed of light. We assume that the function $\varepsilon_r(\mathbf{x})$ satisfies the following conditions:

$$\varepsilon_r(\mathbf{x}) \in C^3(\mathbb{R}^3), \quad (2.11)$$

$$\varepsilon_r(\mathbf{x}) = 1, \quad \mathbf{x} \in \{\mathbf{x} \in \mathbb{R}^3 \mid |x| \geq A, |y| \geq A\} \cup \{\mathbf{x} \in \mathbb{R}^3 \mid z \leq a\}, \quad (2.12)$$

$$\partial_z \varepsilon_r(\mathbf{x}) \geq 0, \quad \mathbf{x} \in \mathbb{R}^3. \quad (2.13)$$

By the Fermat principle, the first time of arrival at the point \mathbf{x} of light generated at the point \mathbf{x}_α is $\tau(\mathbf{x}, \mathbf{x}_0)$ [55, Chapter 3]

$$\tau(\mathbf{x}, \mathbf{x}_0) = \int_{\Gamma(\mathbf{x}, \mathbf{x}_0)} \sqrt{\varepsilon_r(\xi(\sigma))} d\sigma, \quad (2.14)$$

where $d\sigma$ is the element of the Euclidian length. For $\mathbf{x} \neq \mathbf{x}_0$ the function $\tau(\mathbf{x}, \mathbf{x}_0)$ is twice continuously differentiable with respect to \mathbf{x}, \mathbf{x}_0 and is the solution of the eikonal equation [55, Chapter 3]

$$\begin{cases} |\nabla_{\mathbf{x}} \tau(\mathbf{x}, \mathbf{x}_0)|^2 = \varepsilon_r(\mathbf{x}), \\ \tau(\mathbf{x}, \mathbf{x}_0) = O(|\mathbf{x} - \mathbf{x}_0|), \quad \mathbf{x} \rightarrow \mathbf{x}_0. \end{cases} \quad (2.15)$$

We assume everywhere below that the following assumption of regularity of geodesic lines holds [55, Chapter 3]:

Regularity Assumption. Any two points $\mathbf{x}, \mathbf{x}_0 \in \mathbb{R}^3$ can be connected by a single geodesic line $\Gamma(\mathbf{x}, \mathbf{x}_0)$.

A sufficient condition guaranteeing the regularity of geodesic lines can be found in [57]. Let $\mu_a(\mathbf{x})$ and $\mu_s(\mathbf{x})$ be the absorption and scattering coefficients of light respectively. We assume that

$$\mu_a(\mathbf{x}), \mu_s(\mathbf{x}) \geq 0, \quad \mu_a(\mathbf{x}), \mu_s(\mathbf{x}) \in C^1(\mathbb{R}^3), \quad (2.16)$$

$$\mu_a(\mathbf{x}) = \mu_s(\mathbf{x}) = 0, \quad \mathbf{x} \in \mathbb{R}^3 \setminus \Omega. \quad (2.17)$$

6 Convexification method for CIP for RRTE

Denote

$$a(\mathbf{x}) = \mu_a(\mathbf{x}) + \mu_s(\mathbf{x}). \quad (2.18)$$

Then $a(\mathbf{x})$ is the attenuation coefficient. By (2.16)-(2.18)

$$a(\mathbf{x}) \geq 0, \mathbf{x} \in \mathbb{R}^3, a(\mathbf{x}) \in C^1(\mathbb{R}^3), \quad a(\mathbf{x}) = 0, \mathbf{x} \in \mathbb{R}^3 \setminus \Omega. \quad (2.19)$$

Let $\tilde{A} = \max(A, d)$. Introduce three domains G, G_a^+ and G_a^- ,

$$G = \left\{ \mathbf{x} : -\tilde{A} < x, y < \tilde{A}, z \in (0, b) \right\}, G_a^+ = G \cup \{z > a\}, G_a^- = G \setminus G_a^+. \quad (2.20)$$

Below we write sometimes $u(\mathbf{x}, \alpha)$ instead of $u(\mathbf{x}, \mathbf{x}_\alpha)$.

The Forward Problem. Find the solution $u(\mathbf{x}, \alpha) \in C^1(G \times [-d, d])$ of the following problem:

$$\begin{aligned} & \frac{\nabla_{\mathbf{x}} \tau(\mathbf{x}, \mathbf{x}_\alpha)}{\sqrt{\varepsilon_r(\mathbf{x})}} \cdot \nabla_{\mathbf{x}} u(\mathbf{x}, \alpha) + a(\mathbf{x})u(\mathbf{x}, \alpha) = \\ & = \mu_s(\mathbf{x}) \int_{\Gamma_d} K(\mathbf{x}, \alpha, \beta) u(\mathbf{x}, \beta) d\beta + f(\mathbf{x} - \mathbf{x}_\alpha), \quad \mathbf{x} \in G, \mathbf{x}_\alpha \in \Gamma_d, \end{aligned} \quad (2.21)$$

$$u(\mathbf{x}_\alpha, \mathbf{x}_\alpha) = 0 \text{ for } \mathbf{x}_\alpha \in \Gamma_d. \quad (2.22)$$

Definition 2.1. We call equation (2.21) the Riemannian Radiative Transfer Equation (RRTE).

In (2.21), (2.22) $u(\mathbf{x}, \alpha)$ denotes the steady-state radiance at the point \mathbf{x} generated by the source function $f(\mathbf{x} - \mathbf{x}_\alpha)$. The kernel $K(\mathbf{x}, \alpha, \beta)$ of the integral operator in (2.21) is called the ‘‘phase function’’ [24],

$$K(\mathbf{x}, \alpha, \beta) \geq 0, \quad \mathbf{x} \in \bar{\Omega}; \quad \alpha, \beta \in [-d, d], \quad (2.23)$$

$$K(\mathbf{x}, \alpha, \beta) \in C^1(\bar{\Omega} \times [-d, d]^2). \quad (2.24)$$

Coefficient Inverse Problem. Let the function $u(\mathbf{x}, \alpha) \in C^1(\bar{\Omega} \times [-d, d])$ be the solution of the Forward Problem. Assume that the coefficient $a(\mathbf{x})$ of equation (2.21) is unknown. Determine the function $a(\mathbf{x})$, assuming that the following function $g(\mathbf{x}, \alpha)$ is known:

$$g(\mathbf{x}, \alpha) = u(\mathbf{x}, \alpha), \quad \forall \mathbf{x} \in \partial\Omega \setminus \partial_1\Omega, \quad \forall \alpha \in (-d, d). \quad (2.25)$$

3 Existence and Uniqueness Theorem for the Forward Problem

Consider the unit tangent vector ν to the geodesic line $\Gamma(\mathbf{x}, \mathbf{x}_\alpha)$ at the point \mathbf{x} [55, Chapter 3]

$$\nu = \frac{\nabla_{\mathbf{x}} \tau(\mathbf{x}, \mathbf{x}_\alpha)}{\sqrt{\varepsilon_r(\mathbf{x})}}.$$

Hence, the directional derivative of an appropriate function $q(\mathbf{x}, \alpha)$ in the direction of the vector q is

$$D_\nu q = \frac{\nabla_{\mathbf{x}} \tau(\mathbf{x}, \mathbf{x}_\alpha)}{\sqrt{\varepsilon_r(\mathbf{x})}} \cdot \nabla_{\mathbf{x}} q(\mathbf{x}, \alpha). \quad (3.1)$$

Hence, the solution $q(\mathbf{x}, \mathbf{x}_\alpha)$ of the problem

$$\frac{\nabla_{\mathbf{x}} \tau(\mathbf{x}, \mathbf{x}_\alpha)}{\sqrt{\varepsilon_r(\mathbf{x})}} \cdot \nabla_{\mathbf{x}} q(\mathbf{x}, \mathbf{x}_\alpha) = a(\mathbf{x}), \quad q(\mathbf{x}_\alpha, \mathbf{x}_\alpha) = 0 \quad (3.2)$$

is

$$q(\mathbf{x}, \mathbf{x}_\alpha) = \int_{\Gamma(\mathbf{x}, \mathbf{x}_\alpha)} a(\xi(\sigma)) d\sigma. \quad (3.3)$$

Denote

$$p(\mathbf{x}, \mathbf{x}_\alpha) = \exp \left(\int_{\Gamma(\mathbf{x}, \mathbf{x}_\alpha)} a(\xi(\sigma)) d\sigma \right). \quad (3.4)$$

Hence, by (3.1)-(3.4)

$$D_\nu p = a(\mathbf{x}) p. \quad (3.5)$$

Multiply both sides of equation (2.21) by p and use (3.1)-(3.4). Note that by (2.9), (2.17) and (2.18) $p(\mathbf{x}, \mathbf{x}_\alpha) f(\mathbf{x} - \mathbf{x}_\alpha) = f(\mathbf{x} - \mathbf{x}_\alpha)$. We obtain

$$p D_\nu u + a(\mathbf{x}) p u = \mu_s(\mathbf{x}) p \int_{\Gamma_d} K(\mathbf{x}, \alpha, \beta) u(\mathbf{x}, \beta) d\beta + f(\mathbf{x} - \mathbf{x}_\alpha). \quad (3.6)$$

Next,

$$\begin{aligned} p D_\nu u + a(\mathbf{x}) p u &= D_\nu(pu) - u D_\nu p + a(\mathbf{x}) pu \\ &= D_\nu(pu) - a(\mathbf{x}) pu + a(\mathbf{x}) pu = D_\nu(pu). \end{aligned}$$

Hence, (3.6) becomes

$$D_\nu(pu) = \mu_s(\mathbf{x}) p \int_{\Gamma_d} K(\mathbf{x}, \alpha, \beta) u(\mathbf{x}, \beta) d\beta + f(\mathbf{x} - \mathbf{x}_\alpha). \quad (3.7)$$

Let the equation of the geodesic line $\Gamma(\mathbf{x}, \mathbf{x}_\alpha)$ be $\xi = \xi(\sigma, \alpha) \in \Gamma(\mathbf{x}, \mathbf{x}_\alpha)$, where σ is the Euclidean length of the part $\Gamma_\xi(\mathbf{x}, \mathbf{x}_\alpha)$ of the curve $\Gamma(\mathbf{x}, \mathbf{x}_\alpha)$, which connects points ξ and \mathbf{x}_α . Integrating equation (3.7) along the vector ν and taking into account the initial condition (2.22), we obtain for $\mathbf{x} \in G, \mathbf{x}_\alpha \in \Gamma_d$

$$u(\mathbf{x}, \mathbf{x}_\alpha) = u_0(\mathbf{x}, \mathbf{x}_\alpha) + \frac{1}{p(\mathbf{x}, \mathbf{x}_\alpha)} \times$$

8 Convexification method for CIP for RRTE

$$\times \int_{\Gamma(\mathbf{x}, \mathbf{x}_\alpha)} p(\xi(\sigma, \alpha), \mathbf{x}_\alpha) \mu_s(\xi(\sigma, \alpha)) \int_{\Gamma_d} K(\xi(\sigma, \alpha), \alpha, \beta) u(\xi(\sigma, \alpha), \beta) d\beta d\sigma, \quad (3.8)$$

$$u_0(\mathbf{x}, \mathbf{x}_\alpha) = \frac{1}{p(\mathbf{x}, \mathbf{x}_\alpha)} \int_{\Gamma(\mathbf{x}, \mathbf{x}_\alpha)} f(\xi(\sigma, \alpha) - \mathbf{x}_\alpha) d\sigma. \quad (3.9)$$

Theorem 3.1. Assume that conditions (2.16)-(2.18), (2.23) and (2.24) hold. Then there exists unique solution $u(\mathbf{x}, \alpha) \in C^1(G \times [d, d])$ of problem (2.21), (2.22). Furthermore, the following inequality is valid:

$$u(\mathbf{x}, \alpha) \geq m > 0 \text{ for } (\mathbf{x}, \alpha) \in (\overline{G}_a^+ \times [-d, d]), \quad (3.10)$$

$$m = \min_{(\mathbf{x}, \alpha) \in (\overline{G}_a^+ \times [-d, d])} u_0(\mathbf{x}, \alpha), \quad (3.11)$$

where the domain G_a^+ is defined in (2.20).

Proof. Let \mathbf{x}^* be the intersection point of the geodesic line $\Gamma(\mathbf{x}, \mathbf{x}_\alpha)$ with plane $\{z = a\}$. Note that by (2.1), (2.6) and (2.12) $\Gamma(\mathbf{x}^*, \mathbf{x}_\alpha)$ is an interval of a straight line. Since by (2.1), (2.17) and (2.20) $\mu_s(\mathbf{x}) = 0$ for $\mathbf{x} \in G_a^-$, then equation (3.8) can be rewritten as:

$$u(\mathbf{x}, \mathbf{x}_\alpha) = u_0(\mathbf{x}, \mathbf{x}_\alpha) + \frac{1}{p(\mathbf{x}, \mathbf{x}_\alpha)} \int_{\Gamma(\mathbf{x}, \mathbf{x}^*)} \int_{\Gamma_d} \widehat{K}(\xi(\sigma, \alpha), \alpha, \beta) u(\xi(\sigma, \alpha), \beta) d\beta d\sigma, \quad (3.12)$$

where the function $u_0(\mathbf{x}, \mathbf{x}_\alpha)$ is given in (3.9) and

$$\widehat{K}(\mathbf{x}, \alpha, \beta) = p(\mathbf{x}, \mathbf{x}_\alpha) \mu_s(\mathbf{x}) K(\mathbf{x}, \alpha, \beta). \quad (3.13)$$

Consider now equations of the geodesic lines. Denote

$$q_1 = \tau_x(\mathbf{x}, \mathbf{x}_\alpha), q_2 = \tau_y(\mathbf{x}, \mathbf{x}_\alpha), q_3 = \tau_z(\mathbf{x}, \mathbf{x}_\alpha). \quad (3.14)$$

Then formulas (3.4) and (3.7) of [55, Chapter 3] imply that equations of geodesic lines are:

$$\frac{dx}{ds} = \frac{q_1}{\varepsilon_r}, \quad \frac{dy}{ds} = \frac{q_2}{\varepsilon_r}, \quad \frac{dz}{ds} = \frac{q_3}{\varepsilon_r}, \quad (3.15)$$

$$\frac{dq_1}{ds} = \frac{\partial_x \varepsilon_r}{2\varepsilon_r}, \quad \frac{dq_2}{ds} = \frac{\partial_y \varepsilon_r}{2\varepsilon_r}, \quad \frac{dq_3}{ds} = \frac{\partial_z \varepsilon_r}{2\varepsilon_r},$$

where $ds = \sqrt{\varepsilon_r(\mathbf{x}(\sigma))} d\sigma$ is the element of the Riemannian length. In the integral of (3.12)

$$\mathbf{x}(\sigma, \alpha) = (x(\sigma, \alpha), y(\sigma, \alpha), z(\sigma, \alpha)) \in \Omega. \quad (3.16)$$

It follows from (2.13) and [45, Lemma 5.1] that there exists a number $c > 0$ such that

$$\tau_z(\mathbf{x}, \mathbf{x}_\alpha) \geq c. \quad (3.17)$$

Hence, a combination of the last equation of (3.14) with the last equation of (3.15) implies that

$$\partial_s z(s, \alpha) > 0 \text{ and } \partial_\sigma z(\sigma, \alpha) > 0. \quad (3.18)$$

Consider the equation of the geodesic line $\Gamma(\mathbf{x}, \mathbf{x}^*)$ as

$$\xi(\sigma, \alpha) = (\xi(\sigma, \alpha), \eta(\sigma, \alpha), \zeta(\sigma, \alpha)) \quad (3.19)$$

and replace variable σ by $\zeta = \zeta(\sigma, \alpha)$. Let $\sigma = \sigma(\zeta, \alpha)$ be the inverse function. Then the equation of the geodesic line $\Gamma(\mathbf{x}, \mathbf{x}^*)$ can be rewritten as

$$\xi = \widehat{\xi}(\zeta, \alpha) = \xi(\sigma(\zeta, \alpha), \alpha) = (\xi(\sigma(\zeta, \alpha), \alpha), \eta(\sigma(\zeta, \alpha), \alpha), \zeta), \quad \zeta \in (a, z).$$

By (3.16), (3.18) and (3.19) the inverse function $\sigma = \sigma(\zeta, \alpha)$ is monotonically increasing with respect to ζ along the geodesic line $\Gamma(x, x^*)$, i.e. $\partial_\zeta \sigma(\zeta, \alpha) > 0$. Hence, we change variables in the integral of (3.12) as: $\sigma \Leftrightarrow \zeta = \zeta(\sigma, \alpha)$. Then equation (3.12) can be rewritten as:

$$u(\mathbf{x}, \mathbf{x}_\alpha) = u_0(\mathbf{x}, \mathbf{x}_\alpha) + \int_a^z \int_{\Gamma_d} \widetilde{K}(\mathbf{x}, \widehat{\xi}(\zeta, \alpha), \alpha, \beta, \zeta) u(\widehat{\xi}(\zeta, \alpha), \beta) d\beta d\zeta, \quad (3.20)$$

where $\mathbf{x} \in G_a^+$, $\mathbf{x}_\alpha \in \Gamma_d$ and by (3.13)

$$\widetilde{K}(\mathbf{x}, \xi, \alpha, \beta, \zeta) = \frac{1}{p(\mathbf{x}, \mathbf{x}_\alpha)} \widehat{K}(\xi, \alpha, \beta) \partial_\zeta \sigma(\zeta, \alpha). \quad (3.21)$$

Equation (3.20) is the integral equation of the Volterra type. It follows from (2.11), (2.23), (2.24), (3.4), (3.13)-(3.15) and (3.21) that the kernel of equation (3.20) is a non negative continuously differentiable function of its variables $(\mathbf{x}, \alpha, \beta, z) \in (\overline{G}_a^+ \times \overline{\Gamma}_d \times \overline{\Gamma}_d \times [a, b])$. Hence, there exists a number $K_0 > 0$ such that in (3.20), (3.21)

$$0 \leq \widetilde{K}(\mathbf{x}, \xi, \alpha, \beta, \zeta) \leq K_0 < \infty \text{ in (3.20)}. \quad (3.22)$$

Since equation (3.20) is of the Volterra type, then its solution can be obtained iteratively as:

$$u_n(\mathbf{x}, \mathbf{x}_\alpha) = \int_a^z \int_{\Gamma_d} \widetilde{K}(\mathbf{x}, \widehat{\xi}(\zeta, \alpha), \alpha, \beta, \zeta) u_{n-1}(\widehat{\xi}(\zeta, \alpha), \beta) d\beta d\zeta, \quad (3.23)$$

$$u(\mathbf{x}, \mathbf{x}_\alpha) = \sum_{n=0}^{\infty} u_n(\mathbf{x}, \mathbf{x}_\alpha). \quad (3.24)$$

It follows from (2.7), (2.8) and (3.20)-(3.24)

$$\begin{aligned} m &\leq u(\mathbf{x}, \mathbf{x}_\alpha) \leq \\ &\leq \left[\max_{(\mathbf{x}, \alpha) \in (G_d^+ \times [-d, d])} u_0(\mathbf{x}, \mathbf{x}_\alpha) \right] \sum_{n=0}^{\infty} \frac{(2dK_0(z-a))^k}{n!}, \quad \mathbf{x} \in G_a^+, \end{aligned} \quad (3.25)$$

where numbers m and K_0 are defined in (3.11) and (3.22) respectively. Estimate (3.10) follows from (3.25). Obviously the series of first derivatives of terms of (3.24) with respect to any of variables x, y, z, α also converges absolutely. Hence the function $u(\mathbf{x}, \mathbf{x}_\alpha)$ in (3.24) belongs to $C^1(\overline{G}_a^+ \times \overline{\Gamma}_d)$. We set

$$u(\mathbf{x}, \mathbf{x}_\alpha) = \begin{cases} \text{the right hand side of (3.24) for } (\mathbf{x}, \mathbf{x}_\alpha) \in G_a^+ \times \Gamma_d, \\ u_0(\mathbf{x}, \mathbf{x}_\alpha) \text{ for } (\mathbf{x}, \mathbf{x}_\alpha) \in G_a^- \times \Gamma_d. \end{cases}$$

Obviously, the so defined function $u(\mathbf{x}, \mathbf{x}_\alpha) \in C^1(\overline{G} \times \overline{\Gamma}_d)$. Thus, we have proven the existence of the solution $u(\mathbf{x}, \alpha) \in C^1(\overline{G} \times [d, d])$ of the Forward Problem as well as estimate (3.10). To prove uniqueness, one should set in (3.20) $u_0(\mathbf{x}, \mathbf{x}_\alpha) \equiv 0$ and then proceed in the classical way of the proof of the uniqueness of the Volterra integral equation of the second kind. \square

Remark 3.1. *It follows from (3.8), (3.9) and Theorem 3.1 that one can solve Forward Problem via the solution of the linear integral equation (3.8). This is how we solve the forward problem in the numerical section 7 to generate the data for the inverse problem.*

4 Convexification Functional for the Inverse Problem

4.1 An integral differential equation without the unknown coefficient $a(\mathbf{x})$

By (2.7)-(2.9) equation (2.21) can be rewritten as:

$$\begin{aligned} &\frac{\nabla_{\mathbf{x}} \tau(\mathbf{x}, \mathbf{x}_\alpha)}{\sqrt{\varepsilon_r(\mathbf{x})}} \cdot \nabla_{\mathbf{x}} u(\mathbf{x}, \alpha) + a(\mathbf{x})u(\mathbf{x}, \alpha) = \\ &= \mu_s(\mathbf{x}) \int_{\Gamma_d} K(\mathbf{x}, \alpha, \beta) u(\mathbf{x}, \beta) d\beta, \quad (\mathbf{x}, \alpha) \in \Omega \times (-d, d). \end{aligned} \quad (4.1)$$

It follows from (3.10) that we can consider a new function $v(\mathbf{x}, \alpha)$,

$$v(\mathbf{x}, \alpha) = \ln u(\mathbf{x}, \alpha), \quad (\mathbf{x}, \alpha) \in \Omega \times (-d, d). \quad (4.2)$$

By (4.2) $u(\mathbf{x}, \alpha) = e^{v(\mathbf{x}, \alpha)}$. Substituting this in (4.1), we obtain for $(\mathbf{x}, \alpha) \in \Omega \times (-d, d)$:

$$\frac{\nabla_{\mathbf{x}} \tau(\mathbf{x}, \mathbf{x}_\alpha)}{\sqrt{\varepsilon_r(\mathbf{x})}} \cdot \nabla_{\mathbf{x}} v(\mathbf{x}, \alpha) + a(\mathbf{x}) = e^{-v(\mathbf{x}, \alpha)} \mu_s(\mathbf{x}) \int_{\Gamma_d} K(\mathbf{x}, \alpha, \beta) e^{v(\mathbf{x}, \beta)} d\beta. \quad (4.3)$$

In particular, (4.3) implies

$$a(\mathbf{x}) = -\frac{\nabla_{\mathbf{x}} \tau(\mathbf{x}, \mathbf{x}_\alpha)}{\sqrt{\varepsilon_r(\mathbf{x})}} \cdot \nabla_{\mathbf{x}} v(\mathbf{x}, \alpha) + e^{-v(\mathbf{x}, \alpha)} \mu_s(\mathbf{x}) \int_{\Gamma_d} K(\mathbf{x}, \alpha, \beta) e^{v(\mathbf{x}, \beta)} d\beta. \quad (4.4)$$

Hence, we now focus on the problem of the reconstruction of the function $v(\mathbf{x}, \alpha)$ from the function $g(\mathbf{x}, \alpha)$ given in (2.25). We have

$$\frac{\tau_z(\mathbf{x}, \alpha)}{\sqrt{\varepsilon_r(\mathbf{x})}} v_z(\mathbf{x}, \alpha) = \frac{\partial}{\partial z} \left(\frac{\tau_z}{\sqrt{\varepsilon_r}} v \right) - \frac{\partial}{\partial z} \left(\frac{\tau_z}{\sqrt{\varepsilon_r}} \right) v. \quad (4.5)$$

Introduce a new function

$$w(\mathbf{x}, \alpha) = \frac{\tau_z(\mathbf{x}, \alpha)}{\sqrt{\varepsilon_r(\mathbf{x})}} v(\mathbf{x}, \alpha). \quad (4.6)$$

Then

$$v(\mathbf{x}, \alpha) = \frac{\sqrt{\varepsilon_r(\mathbf{x})}}{\tau_z(\mathbf{x}, \alpha)} w(\mathbf{x}, \alpha) \quad (4.7)$$

It follows from (3.17) that formula (4.7) makes sense. Thus, (4.5) becomes

$$\frac{\tau_z}{\sqrt{\varepsilon_r}} v_z = w_z - \left[\frac{\partial}{\partial z} \left(\frac{\tau_z}{\sqrt{\varepsilon_r}} \right) \frac{\sqrt{\varepsilon_r}}{\tau_z} \right] w. \quad (4.8)$$

Using (4.6) and (4.7), transform other terms of the differential operator in (4.3),

$$\frac{\tau_x}{\sqrt{\varepsilon_r}} v_x = \frac{\tau_x}{\sqrt{\varepsilon_r}} \frac{\partial}{\partial x} \left(\frac{\sqrt{\varepsilon_r}}{\tau_z} w \right) = \frac{\tau_x}{\tau_z} w_x + \left[\frac{\tau_x}{\sqrt{\varepsilon_r}} \frac{\partial}{\partial x} \left(\frac{\sqrt{\varepsilon_r}}{\tau_z} \right) \right] w. \quad (4.9)$$

And similarly for $(\tau_y/\sqrt{\varepsilon_r}) v_y$. Hence, (4.3) becomes

$$\left\{ \begin{array}{l} w_z + \frac{1}{\tau_z} (\tau_x w_x + \tau_y w_y) + \\ + \left[\frac{\tau_x}{\sqrt{\varepsilon_r}} \frac{\partial}{\partial x} \left(\frac{\sqrt{\varepsilon_r}}{\tau_z} \right) + \frac{\tau_y}{\sqrt{\varepsilon_r}} \frac{\partial}{\partial y} \left(\frac{\sqrt{\varepsilon_r}}{\tau_z} \right) - \frac{\partial}{\partial z} \left(\frac{\tau_z}{\sqrt{\varepsilon_r}} \right) \frac{\sqrt{\varepsilon_r}}{\tau_z} \right] w \\ - \exp \left(-\frac{\sqrt{\varepsilon_r}}{\tau_z} w \right) (\mathbf{x}, \alpha) \mu_s(\mathbf{x}) \int_{\Gamma_d} K(\mathbf{x}, \alpha, \beta) \exp \left(\frac{\sqrt{\varepsilon_r}}{\tau_z} w \right) (\mathbf{x}, \beta) d\beta = \\ = -a(\mathbf{x}), \quad (\mathbf{x}, \alpha) \in \Omega \times (-d, d). \end{array} \right. \quad (4.10)$$

Differentiate both sides of (4.10) with respect to α and use $\partial_\alpha a(\mathbf{x}) \equiv 0$. We obtain the following integral differential equation with the derivatives up to the second order for $(\mathbf{x}, \alpha) \in \Omega \times (-d, d)$:

$$\left\{ \begin{aligned} & \partial_\alpha w_z + \frac{\partial}{\partial \alpha} \left(\frac{1}{\tau_z} (\tau_x w_x + \tau_y w_y) \right) + \frac{\partial}{\partial \alpha} \left[\sum_{i=1}^n \left(\frac{\tau_{x_i}}{\sqrt{c}} \frac{\partial}{\partial x_i} \left(\frac{\sqrt{c}}{\tau_y} \right) \right) w \right] + \\ & + \frac{\partial}{\partial \alpha} \left\{ \left[\frac{\tau_x}{\sqrt{\varepsilon_r}} \frac{\partial}{\partial x} \left(\frac{\sqrt{\varepsilon_r}}{\tau_z} \right) + \frac{\tau_y}{\sqrt{\varepsilon_r}} \frac{\partial}{\partial y} \left(\frac{\sqrt{\varepsilon_r}}{\tau_z} \right) - \frac{\partial}{\partial z} \left(\frac{\tau_z}{\sqrt{\varepsilon_r}} \right) \frac{\sqrt{\varepsilon_r}}{\tau_z} \right] w \right\} - \\ & - \frac{\partial}{\partial \alpha} \left[e^{-\frac{\sqrt{\varepsilon_r}}{\tau_z} w(\mathbf{x}, \alpha)} \mu_s(\mathbf{x}) \int_{\Gamma_d} K(\mathbf{x}, \alpha, \beta) e^{\frac{\sqrt{\varepsilon_r}}{\tau_z} w(\mathbf{x}, \beta)} d\beta \right] = 0. \end{aligned} \right. \quad (4.11)$$

The Dirichlet boundary condition for the function $w(\mathbf{x}, \alpha)$ is:

$$w(\mathbf{x}, \alpha) = \frac{\tau_z(\mathbf{x}, \alpha)}{\sqrt{\varepsilon_r(\mathbf{x})}} \ln g_1(\mathbf{x}, \alpha), \quad (\mathbf{x}, \alpha) \in \partial\Omega \times (-d, d), \quad (4.12)$$

$$g_1(\mathbf{x}, \alpha) = \begin{cases} g(\mathbf{x}, \alpha), & \mathbf{x} \in \partial\Omega \setminus \partial_1\Omega, \quad \alpha \in (-d, d), \\ u_0(\mathbf{x}, \alpha), & \mathbf{x} \in \partial_1\Omega, \quad \alpha \in (-d, d). \end{cases} \quad (4.13)$$

Thus, we develop below a numerical method to obtain an approximate solution $w(\mathbf{x}, \alpha)$ of problem (4.11)-(4.13).

4.2 A special orthonormal basis in $L_2(-d, d)$

We now introduce a special orthonormal basis in $L_2(-d, d)$, which was first discovered in [39], also, see [43, section 6.2.3]. Consider a linearly independent set of functions $\{\alpha^n e^\alpha\}_{n=0}^\infty \subset L_2(-d, d)$, which is complete in $L_2(-d, d)$. The Gram-Schmidt orthonormalization procedure being applied to this set, results in the orthonormal basis $\{\Psi_n(\alpha)\}_{n=0}^\infty$ in $L_2(-d, d)$. The Gram-Schmidt procedure is unstable when it is applied to an infinite number of functions. However, we have not seen an instability when applying it to a relatively small number of functions for $n \in [0, 12]$. The same was observed in a number of other works of this research group, see, e.g. [30, 31, 46], [43, Chapters 7,10,12].

Let $[\cdot, \cdot]$ be the scalar product in $L_2(-d, d)$. Denote $b_{s,k} = [Q'_s, Q_k]$. Then [39], [43, section 6.2.3]

$$b_{s,k} = \begin{cases} 1, & s = k, \\ 0, & s > k. \end{cases} \quad (4.14)$$

Consider the $N \times N$ matrix $B_N = (b_{s,k})_{(s,k)=(0,0)}^{(N-1,N-1)}$. Then (4.14) implies that $\det B_N = 1$, which means that this matrix is invertible. In fact, the existence of the matrix B_N^{-1} for each $N \geq 1$ is the key property why the basis $\{Q_n(\alpha)\}_{n=0}^\infty$ was originally constructed in [39]. Indeed, consider, for example either the basis of standard orthonormal polynomials or the basis of trigonometric functions. In each of these, the first function is an identical constant, which means that the first row of an analog of the matrix B_N is zero.

4.3 A boundary value problem for a system of nonlinear equations

We assume that the functions $w(\mathbf{x}, \alpha), w_\alpha(\mathbf{x}, \alpha)$ can be represented as truncated Fourier-like series

$$w(\mathbf{x}, \alpha) = \sum_{n=0}^{N-1} w_n(\mathbf{x}) Q_n(\alpha), \quad w_\alpha(\mathbf{x}, \alpha) = \sum_{n=0}^{N-1} w_n(\mathbf{x}) Q'_n(\alpha) \quad (4.15)$$

with unknown coefficients $\{w_n(\mathbf{x})\}_{n=0}^{N-1}$. Thus, we focus below on the computation of the N -D vector function

$$V(\mathbf{x}) = (w_0, w_1, \dots, w_{N-1})^T(\mathbf{x}).$$

Remark 4.1. *The representations (4.15) mean that this is a version of the Galerkin method. However, unlike classical well-posed forward problems for PDEs, where Galerkin method is used and its convergence at $N \rightarrow \infty$ is usually proven, we cannot prove convergence of our inversion numerical procedure described below for $N \rightarrow \infty$. This is basically because of the ill-posed nature of our CIP. Thus, we actually work below within the framework of an approximate mathematical model. Then, however, the question can be raised whether this model really works numerically. The answer is positive, and this answer is obtained computationally in section 7. We observe that very similar truncated series were used in some other above cited works on the convexification, such as, e.g. [30, 31, 46], [43, Chapters 7,10], and all of them have demonstrated good numerical performances, including the quite challenging cases of experimentally collected data for backscatter microwaves [31], [43, Chapter 10]. Likewise, truncated Fourier series were used in works of other authors about CIPs, such as, e.g. [22, 28, 29, 53] and also without proofs of convergence of inversion procedures at $N \rightarrow \infty$. Those proofs were not provided for the same reason as the one here: the ill-posed nature of CIPs. Finally, we refer to subsection 3.4 of [46] for a detailed discussion of this issue for the case of a similar CIP for the conventional RTE.*

Substitute (4.15) in (4.11). Next, sequentially multiply the obtained equation by $Q_n(\alpha), n = 0, \dots, N - 1$ and integrate with respect to $\alpha \in (-d, d)$. We obtain the following system of coupled quasilinear integral differential equations

$$B_N V_z(\mathbf{x}) + A_1(\mathbf{x}) V_x(\mathbf{x}) + A_2(\mathbf{x}) V_y(\mathbf{x}) + F(V(\mathbf{x}), \mathbf{x}) = 0, \quad \mathbf{x} \in \Omega. \quad (4.16)$$

In addition, the boundary condition for the vector function $V(\mathbf{x})$ is:

$$V(\mathbf{x})|_{\partial\Omega} = P(\mathbf{x}) = (p_0, p_1, \dots, p_{N-1})^T(\mathbf{x}), \quad (4.17)$$

$$p_n(\mathbf{x}) = \int_{-d}^d \left[\frac{\tau_z(\mathbf{x}, \alpha)}{\sqrt{\varepsilon_r(\mathbf{x})}} \ln [g_1(\mathbf{x}, \alpha)] \right] Q_n(\alpha) d\alpha, \quad n = 0, 1, \dots, N-1. \quad (4.18)$$

Thus, we now have to solve the boundary value problem (4.16)-(4.18).

To write explicit formulas for matrices $A_1(\mathbf{x}), A_2(\mathbf{x})$ and for the nonlinear term $F(V(\mathbf{x}), \mathbf{x})$ in (4.16), temporary denote for brevity $x = x_1, y = x_2$. Then in (4.16) for $i = 1, 2$

$$\left\{ \begin{array}{l} A_i(\mathbf{x}) = \left(A_{i,k,s} \right)_{\substack{(N-1, N-1) \\ (k,s)=(0,0)}}, \\ A_i(\mathbf{x}) = \left(A_{i,k,s} \right)_{\substack{(N-1, N-1) \\ (k,s)=(0,0)}}, \\ A_{i,k,s} = \int_{-d}^d \left[\frac{\partial}{\partial \alpha} \left(\frac{\tau_{x_i}}{\tau_z} \right) Q_s + \frac{\tau_{x_i}}{\tau_z} Q'_s \right] Q_k(\alpha) d\alpha, \end{array} \right. \quad (4.19)$$

$$\left\{ \begin{array}{l} F(V(\mathbf{x}), \mathbf{x}) = \sum_{i=1}^2 F_i(\mathbf{x})V(\mathbf{x}) + F^{(z)}(\mathbf{x})V(\mathbf{x}) + F_0(V(\mathbf{x}), \mathbf{x}), \\ F_i(\mathbf{x}) = \left(F_{i,k,s}(\mathbf{x}) \right)_{\substack{(N-1, N-1) \\ (k,s)=(0,0)}}, \quad i = 1, 2; \\ F^{(z)}(\mathbf{x}) = \left(F_{k,s}^{(z)} \right)_{\substack{(N-1, N-1) \\ (k,s)=(0,0)}}, \\ F_0(V(\mathbf{x}), \mathbf{x}) = \left(F_{0,k}(\mathbf{x}) \right)_{k=0}^{N-1}, \\ F_{i,k,s}(\mathbf{x}) = \\ = \int_{-d}^d \left\{ \frac{\partial}{\partial \alpha} \left[\frac{\tau_{x_i}}{\sqrt{\varepsilon_r}} \frac{\partial}{\partial x_i} \left(\frac{\sqrt{\varepsilon_r}}{\tau_z} \right) \right] Q_s + \frac{\tau_{x_i}}{\sqrt{\varepsilon_r}} \frac{\partial}{\partial x_i} \left(\frac{\sqrt{\varepsilon_r}}{\tau_z} \right) Q'_s \right\} Q_k(\alpha) d\alpha, \\ F_{k,s}^{(z)}(\mathbf{x}) = \\ = - \int_{-d}^d \left\{ \frac{\partial}{\partial \alpha} \left[\frac{\partial}{\partial y} \left(\frac{\tau_z}{\sqrt{\varepsilon_r}} \right) \frac{\sqrt{\varepsilon_r}}{\tau_z} \right] Q_s + \left[\frac{\partial}{\partial z} \left(\frac{\tau_z}{\sqrt{\varepsilon_r}} \right) \frac{\sqrt{\varepsilon_r}}{\tau_z} \right] Q'_s \right\} Q_k(\alpha) d\alpha, \\ F_{0,k}(\mathbf{x}) = \\ = -\mu_s(\mathbf{x}) \int_{-d}^d \frac{\partial}{\partial \alpha} \left[r(\mathbf{x}, \alpha) \int_{\Gamma_d} K(\mathbf{x}, \alpha, \beta) r^{-1}(\mathbf{x}, \beta) d\beta \right] Q_k(\alpha) d\alpha, \\ r(\mathbf{x}, \alpha) = \exp \left(-\frac{\sqrt{\varepsilon_r}}{\tau_z}(\mathbf{x}) \sum_{n=0}^{N-1} w_n(\mathbf{x}) Q_n(\alpha) \right). \end{array} \right. \quad (4.20)$$

To numerically calculate the derivatives of $\nabla_{\mathbf{x}}\tau(\mathbf{x}, \alpha)$ with respect to α , we represent $\nabla_{\mathbf{x}}\tau(\mathbf{x}, \alpha)$ via the truncated Fourier series with respect to the above basis $\{Q_n(\alpha)\}_{n=0}^{N-1}$ as

$$\nabla_{\mathbf{x}}\tau(\mathbf{x}, \alpha) = \sum_{n=0}^{N-1} (\nabla_{\mathbf{x}}\tau)_n(\mathbf{x})Q_n(\alpha). \quad (4.21)$$

Then we use explicit formulas for functions $Q_n(\alpha)$ to get

$$\partial_\alpha (\nabla_{\mathbf{x}} \tau) = \sum_{n=0}^{N-1} (\nabla_{\mathbf{x}} \tau)_s(\mathbf{x}) Q'_n(\alpha). \quad (4.22)$$

Then equations (4.21) and (4.22) are used in (4.19) and (4.20). Thus, it follows from (4.19)-(4.22) that

$$\left\{ \begin{array}{l} A_1(\mathbf{x}), A_2(\mathbf{x}) \in C_{N^2}(\overline{\Omega}), \text{ and the vector function} \\ F(V(\mathbf{x}), \mathbf{x}) \text{ is continuously differentiable} \\ \text{with respect to its arguments for } \mathbf{x} \in \overline{\Omega}. \end{array} \right. \quad (4.23)$$

Here and below for any integer $k \geq 2$ and for any Banach space B we denote $B_k = B^k$ with the norm

$$\|f\|_{B_k} = \left(\sum_{i=1}^k \|f_i\|_B^2 \right)^{1/2}, \quad \forall f = (f_1, \dots, f_k)^T \in B_k.$$

4.4 Minimization problem

Let $R > 0$ be an arbitrary number and the vector function $P(x)$ be the boundary condition in (4.17). Define the set $S(R, P) \subset H_N^1(\Omega)$ as:

$$S(R, P) = \left\{ V \in H_N^1(\Omega) : V(\mathbf{x})|_{\partial\Omega} = P(\mathbf{x}), \|W\|_{H_N^1(\Omega)} < R \right\}. \quad (4.24)$$

To solve problem (4.16)-(4.18), we solve the following minimization problem:

Minimization Problem 1. *Let $\lambda \geq 1$ be a parameter. Minimize the following weighted cost functional $J_\lambda(V)$ on the set $S(R, P)$:*

$$\begin{aligned} J_\lambda(V) = \\ = \left\| (B_N V_z + A_1(\mathbf{x}) V_x(\mathbf{x}) + A_2(\mathbf{x}) V_y(\mathbf{x}) + F(V(\mathbf{x}), \mathbf{x})) e^{\lambda z} \right\|_{L_N^2(\Omega)}^2. \end{aligned} \quad (4.25)$$

Remark 4.1. *The function $\varphi_\lambda(z) = e^{2\lambda z}$ is the Carleman Weight Function for the semidiscrete version of the functional $J_\lambda(V)$, see subsection 4.5 for the semidiscrete version and Theorem 5.1 in section 5 for a Carleman estimate.*

To conduct the convergence analysis for a modified Minimization Problem 1, we need to rewrite the differential operator in functional (4.25) via finite differences with respect to the variables x, y while leaving the conventional derivative with respect to z .

4.5 Partial finite differences

Let $m > 1$ be an integer. Let $A > 0$ be the number in (2.2). Consider two partitions of the interval $(-A, A)$,

$$-A = x_0 < x_1 < \cdots < x_m = A, \quad x_{j+1} - x_j = h, \quad j = 0, \dots, m-1, \quad (4.26)$$

$$-A = y_0 < y_1 < \cdots < y_m = A, \quad y_{j+1} - y_j = h, \quad j = 0, \dots, m-1. \quad (4.27)$$

We assume that

$$h \geq h_0 = \text{const.} > 0. \quad (4.28)$$

Define the semidiscrete subset Ω^h of the domain Ω as:

$$\Omega_1^h = \{(x_i, y_j)\}_{i,j=0}^m, \quad (4.29)$$

$$\Omega^h = \Omega_1^h \times (a, b) = \{(x_i, y_j) : (x_i, y_j) \in \Omega_1^h, z \in (a, b)\}. \quad (4.30)$$

Below points $(x_i, y_j, z) \in \Omega^h$ are denoted as \mathbf{x}^h . By (2.2)-(2.5), (4.29) and (4.30) the boundary $\partial\Omega^h$ of the domain Ω^h is:

$$\begin{aligned} \partial\Omega^h &= \partial_1\Omega^h \cup \partial_2\Omega^h \cup \partial_3\Omega^h, \\ \partial_1\Omega^h &= \Omega_1^h \times \{z = a\}, \quad \partial_2\Omega^h = \Omega_1^h \times \{z = b\}, \\ \partial_3\Omega^h &= \{(x_0, y_j, z), (x_m, y_j, z) : z \in (a, b)\}. \end{aligned}$$

Let the vector function $Y(\mathbf{x}) \in C_N^1(\overline{\Omega})$. Denote

$$Y^h(\mathbf{x}^h) = Y(x_i, y_j, z), \quad \mathbf{x}^h = (x_i, y_j, z) \in \Omega^h.$$

Thus, $Y^h(\mathbf{x}^h)$ is an $N - D$ vector function of discrete variables $(x_i, y_j) \in \Omega_1^h$ and continuous variable $z \in (a, b)$. Note that by (4.26) and (4.27) the boundary terms at $\partial_3\Omega^h$ of this vector function, which correspond to $Y(\mathbf{x})|_{\partial_3\Omega^h}$, are:

$$\{Y(x_0, y_j, z)\} \cup \{Y(x_m, y_j, z)\} \cup \{Y(x_i, y_0, z)\} \cup \{Y(x_i, y_m, z)\}, \quad i, j = 0, \dots, m.$$

For two vector functions $Y^{(1)}(\mathbf{x}) = \left(Y_0^{(1)}(\mathbf{x}), \dots, Y_{N-1}^{(1)}(\mathbf{x})\right)^T$ and $Y^{(2)}(\mathbf{x}) = \left(Y_0^{(2)}(\mathbf{x}), \dots, Y_{N-1}^{(2)}(\mathbf{x})\right)^T$ their scalar product $Y^{(1)}(\mathbf{x}) \cdot Y^{(2)}(\mathbf{x})$ is defined as the scalar product in \mathbb{R}^N , and $(Y(\mathbf{x}))^2 = Y(\mathbf{x}) \cdot Y(\mathbf{x})$. Respectively

$$\begin{aligned} & Y^{(1)h}(\mathbf{x}^h) \cdot Y^{(2)h}(\mathbf{x}^h) \\ &= \sum_{n=0}^{N-1} \sum_{(i,j)=(1,1)}^{(i,j)=(m-1,m-1)} Y_n^{(1)h}(x_i, y_j, z) Y_n^{(2)h}(x_i, y_j, z), \end{aligned} \quad (4.31)$$

$$(Y^h(\mathbf{x}^h))^2 = Y^h(\mathbf{x}^h) \cdot Y^h(\mathbf{x}^h), \quad |Y^h(\mathbf{x}^h)| = \sqrt{Y^h(\mathbf{x}^h) \cdot Y^h(\mathbf{x}^h)}. \quad (4.32)$$

We will use formulas (4.31), (4.32) everywhere below without further mentioning. We exclude here boundary terms with $i, j = 0$ and $i, j = m$ since we work below with finite difference derivatives as defined in the next paragraph.

We define finite difference derivatives of the semidiscrete N -D vector function $Y^h(\mathbf{x}^h)$ with respect to x, y only at interior points of the domain Ω^h with $i, j = 1, \dots, m-1$,

$$\partial_x Y^h(x_i, y_j, z) = Y^h(x_i, y_j, z)_x = \frac{Y^h(x_{i+1}, y_j, z) - Y^h(x_{i-1}, y_j, z)}{2h}, \quad (4.33)$$

$$\partial_y Y^h(x_i, y_j, z) = Y^h(x_i, y_j, z)_y = \frac{Y^h(x_i, y_{j+1}, z) - Y^h(x_i, y_{j-1}, z)}{2h}, \quad (4.34)$$

$$Y_x^h(\mathbf{x}^h) = \{Y^h(x_i, y_j, z)\}_{i,j=1}^{m-1}, \quad Y_y^h(\mathbf{x}^h) = \{Y^h(x_i, y_j, z)\}_{i,j=1}^{m-1}. \quad (4.35)$$

We need semidiscrete analogs of spaces $C_{N^2}(\overline{\Omega})$, $H_N^1(\Omega)$, $L_N^2(\Omega)$. All three are defined using the same principle. Hence, we provide here only two definitions: for the space $H_N^{1,h}(\Omega^h)$ and its subspace $H_{N,0}^{1,h}(\Omega^h)$. Others are similar. We introduce the space $H_N^{1,h}(\Omega^h)$ as:

$$H_N^{1,h}(\Omega^h) = \left\{ Y^h(\mathbf{x}^h) : \|Y^h(\mathbf{x}^h)\|_{H_N^{1,h}(\Omega^h)}^2 = \sum_{i,j=1}^{m-1} \int_a^b (Y^h(x_i, y_j, z))^2 dz + \sum_{i,j=1}^{m-1} \int_a^b (Y_x^h(x_i, y_j, z))^2 dz + \sum_{i,j=1}^{m-1} \int_a^b (Y_y^h(x_i, y_j, z))^2 dz + \sum_{i,j=1}^{m-1} \int_a^b (Y_z^h(x_i, y_j, z))^2 dz < \infty \right\}, \quad (4.36)$$

$$H_{N,0}^{1,h}(\Omega^h) = \left\{ Y^h(\mathbf{x}^h) \in H_N^{1,h}(\Omega^h) : Y^h(\mathbf{x}^h)|_{\partial\Omega^h} = 0 \right\}. \quad (4.37)$$

By embedding theorem $H_N^{1,h}(\Omega^h) \subset C_N^h(\overline{\Omega}^h)$ and

$$\|Y^h(\mathbf{x}^h)\|_{C_N^h(\overline{\Omega}^h)} \leq C \|Y^h(\mathbf{x}^h)\|_{H_N^{1,h}(\Omega^h)}, \quad \forall Y^h \in H_N^{1,h}(\Omega^h), \quad (4.38)$$

where the number $C = C(h_0, A, \Omega) > 0$ depends only on listed parameters, where h_0 is defined in (4.28). Also, it follows from (4.28), (4.33)-(4.35) that

$$\|Y_x^h(\mathbf{x}^h)\|_{L^{2,h}(\Omega^h)}, \|Y_y^h(\mathbf{x}^h)\|_{L^{2,h}(\Omega^h)} \leq C \|Y^h(\mathbf{x}^h)\|_{L^{2,h}(\Omega^h)}. \quad (4.39)$$

The following formulas are semidiscrete analogs of (4.15):

$$w^h(\mathbf{x}^h, \alpha) = \sum_{n=0}^{N-1} w_n^h(\mathbf{x}^h) Q_n(\alpha), \quad \partial_\alpha w^h(\mathbf{x}^h, \alpha) = \sum_{n=0}^{N-1} w_n^h(\mathbf{x}^h) Q'_n(\alpha). \quad (4.40)$$

Also, let $V^h(\mathbf{x}^h) = (w_0^h, \dots, w_{N-1}^h)^T(\mathbf{x}^h)$. Using (4.33)-(4.35) and (4.40), we now rewrite problem (4.16)-(4.18), in the form of partial finite differences as:

$$B_N V_z^h(\mathbf{x}^h) + A_1^h(\mathbf{x}^h) V_x^h(\mathbf{x}^h) + A_2^h(\mathbf{x}^h) V_y^h(\mathbf{x}^h) + F^h(V^h(\mathbf{x}^h), \mathbf{x}^h) = 0, \quad \mathbf{x}^h \in \Omega^h, \quad (4.41)$$

$$V^h(\mathbf{x}^h)|_{\partial\Omega^h} = P^h(\mathbf{x}^h). \quad (4.42)$$

Suppose that we have found the vector function $V^h(\mathbf{x}^h)$ satisfying equation (4.41) and boundary condition (4.42). Let $r^h(\mathbf{x}^h, \alpha)$ be the semidiscrete analog of the function $r(\mathbf{x}, \alpha)$ given in the last line of (4.20). Then (4.4) and (4.6) imply that to find the semidiscrete analog $a^h(\mathbf{x}^h)$ of the unknown coefficient $a(\mathbf{x})$, we should use:

$$a^h(\mathbf{x}^h) = -\frac{1}{2d} \int_{-d}^d \frac{\nabla_{\mathbf{x}^h} \tau^h(\mathbf{x}^h, \alpha)}{\sqrt{\varepsilon_r^h(\mathbf{x}^h)}} \cdot \nabla_{\mathbf{x}^h} \left(\frac{\tau_z^h(\mathbf{x}^h, \mathbf{x}_\alpha^h)}{\sqrt{\varepsilon_r^h(\mathbf{x}^h)}} w^h(\mathbf{x}^h, \alpha) \right) d\alpha + \frac{1}{2d} \int_{-d}^d \left(r^h(\mathbf{x}^h, \alpha) \mu_s(\mathbf{x}^h) \int_{-d}^d K(\mathbf{x}^h, \alpha, \beta) (r^h(\mathbf{x}^h, \beta))^{-1} d\beta \right) d\alpha, \quad \mathbf{x}^h \in \Omega^h. \quad (4.43)$$

Obviously, the following semidiscrete analog of (4.23) is valid:

$$\left\{ \begin{array}{l} A_1^h(\mathbf{x}^h), A_2^h(\mathbf{x}^h) \in C_{N^2}^h(\overline{\Omega}^h) \text{ and the vector function} \\ F^h(V^h(\mathbf{x}^h), \mathbf{x}^h) \text{ is continuously differentiable} \\ \text{with respect to its arguments for } \mathbf{x}^h \in \overline{\Omega}^h. \end{array} \right. \quad (4.44)$$

Let $M^h = \max \left(\|A_1^h(\mathbf{x}^h)\|_{C_{N^2}^h}, \|A_2^h(\mathbf{x}^h)\|_{C_{N^2}^h} \right)$. Then

$$M^h \leq M = \max \left(\|A_1(\mathbf{x}^h)\|_{C_{N^2}^h}, \|A_2(\mathbf{x}^h)\|_{C_{N^2}^h} \right). \quad (4.45)$$

The following functional $J_\lambda^h(V^h)$ is the semidiscrete analog of the functional $J_\lambda(V)$ in (4.25):

$$\begin{aligned} J_\lambda^h(V^h) &= \\ &= \left\| (B_N V_z^h + A_1^h V_x^h + A_2^h V_y^h + F^h(V^h(\mathbf{x}^h), \mathbf{x}^h)) e^{\lambda z} \right\|_{L_{N^2}^{2,h}(\Omega^h)}^2. \end{aligned} \quad (4.46)$$

Let $R > 0$ be an arbitrary number. Define the semidiscrete analog $S^h(R, P^h)$ of the set $S(R, P)$ in (4.24) as:

$$S^h(R, P^h) = \left\{ V^h \in H_N^{1,h}(\Omega^h) : V^h(\mathbf{x}^h)|_{\partial\Omega^h} = P^h(\mathbf{x}^h), \|V^h\|_{H_N^{1,h}(\Omega^h)} < R \right\}. \quad (4.47)$$

To find an approximate solution $V^h(\mathbf{x}^h)$ of problem (4.41), (4.42), we consider the following problem:

Minimization Problem 2. Minimize the functional $J_\lambda^h(V^h)$ in (4.46) on the set $\overline{S^h(R, P^h)}$ defined in (4.47).

5 Convergence Analysis

In this section we formulate theorems, which end up with a guarantee of the global convergence property of the gradient descent method of the minimization of functional (4.46) on set (4.47). Proofs of these theorems are provided in section 6.

Lemma 5.1. Consider an $n \times n$ matrix D and assume that the inverse matrix D^{-1} exists. Then there exists a number $\xi = \xi(D) > 0$ such that $\|Dx\|^2 \geq \xi \|x\|^2, \forall x \in R^n$, where $\|\cdot\|$ is the euclidean norm.

We omit the proof of this lemma since it is well known.

Theorem 5.1. (Carleman estimate). Let M be the number defined in (4.45). Assume that (4.28) holds. There exists a sufficiently large number $\lambda_0 = \lambda_0(d, M, \Omega^h, B_N, \tau^h, \varepsilon_r^h, h_0) \geq 1$ depending only on listed parameters such that the following Carleman estimate holds

$$\left\{ \begin{array}{l} \|(B_N V_z^h + A_1^h V_x^h + A_2^h V_y^h) e^{\lambda z}\|_{L_N^{2,h}(\Omega^h)}^2 \geq \\ \geq (1/4) \cdot \|(B_N V_z^h) e^{\lambda z}\|_{L_N^{2,h}(\Omega^h)}^2 + (\lambda^2/8) \cdot \|(B_N V^h) e^{\lambda z}\|_{L_N^{2,h}(\Omega^h)}^2, \\ \forall V^h \in H_{N,0}^{1,h}(\Omega^h), \forall \lambda \geq \lambda_0. \end{array} \right. \quad (5.1)$$

Theorem 5.2 (the central analytical result). Assume that (4.28) holds and let $S^h(R, P^h)$ be the set defined in (4.47). Then:

1. At every point $V^h \in \overline{S^h(R, P^h)}$ and for every $\lambda \geq 0$ the functional $J_\lambda^h(V^h)$ defined in (4.46) has the Fréchet derivative $(J_\lambda^h)'(V^h) \in H_{N,0}^{1,h}(\Omega^h)$. Furthermore, the Fréchet derivative $(J_\lambda^h)'(V^h)$ satisfies the Lipschitz condition

$$\left\| (J_\lambda^h)'(V_2^h) - (J_\lambda^h)'(V_1^h) \right\|_{H_N^{1,h}(\Omega^h)} \leq \rho \|V_2^h - V_1^h\|_{H_N^{1,h}(\Omega^h)}, \quad (5.2)$$

$$\forall V_1^h, V_2^h \in \overline{S^h(R, P^h)},$$

where the number $\rho > 0$ is independent on V_1^h, V_2^h .

2. There exists a sufficiently large number λ_1

$$\lambda_1 = \lambda_1 (R, d, M, \Omega^h, B_N, \tau^h, \varepsilon_r^h, h_0) \geq \lambda_0 \geq 1 \quad (5.3)$$

depending only on listed parameters such that functional (4.46) is strictly convex on the set $\overline{S(R, P^h)}$, i.e. there exists a number

$$C_1 = C_1 (R, d, M, \Omega^h, B_N, \tau^h, \varepsilon_r^h, h_0) > 0 \quad (5.4)$$

depending only on listed parameters such that the following inequality holds:

$$\begin{aligned} J_\lambda^h (V_2^h) - J_\lambda^h (V_1^h) - (J_\lambda^h)' (V_1^h) (V_2^h - V_1^h) &\geq \\ &\geq C_1 \lambda^2 e^{2\lambda a} \|V_2^h - V_1^h\|_{H_N^{1,h}(\Omega^h)}^2, \end{aligned} \quad (5.5)$$

$$\forall \lambda \geq \lambda_1, \forall V_1^h, V_2^h \in \overline{S^h(R, P^h)}. \quad (5.6)$$

3. For each $\lambda \geq \lambda_1$ there exists unique minimizer $V_{\min, \lambda}^h \in \overline{S^h(R, P^h)}$ of the functional $J_\lambda^h (V^h)$ on the set $\overline{S^h(R, P^h)}$ and

$$(J_\lambda^h)' (V_{\min, \lambda}^h) (V^h - V_{\min, \lambda}^h) \geq 0, \forall V^h \in \overline{S^h(R, P^h)}. \quad (5.7)$$

Remark 5.1. Below $C_1 > 0$ denotes different numbers depending on the same parameters as ones listed in (5.4).

Let $\delta > 0$ be the level of the noise in the data. Our goal now is to estimate the accuracy of the minimizer $V_{\min, \lambda}^h$ depending on δ . Following the classical concept for ill-posed problems [62], we assume the existence of the exact solution

$$V^{h*} \in S^h(R, P^{h*}) \quad (5.8)$$

of problem (4.41)-(4.42) with the exact, i.e. noiseless data P^{h*} . Hence,

$$\begin{aligned} B_N V_z^{h*}(\mathbf{x}^h) + A_1^h(\mathbf{x}^h) V_x^{h*}(\mathbf{x}^h) + A_2^h(\mathbf{x}^h) V_x^{h*}(\mathbf{x}^h) + \\ + F^h(V^{h*}(\mathbf{x}^h), \mathbf{x}^h) = 0, \mathbf{x}^h \in \Omega^h, \end{aligned} \quad (5.9)$$

$$V^{h*}(\mathbf{x}^h) |_{\partial\Omega^h} = P^{h*}(\mathbf{x}^h). \quad (5.10)$$

Let two vector functions $G^{h*}(\mathbf{x}^h)$ and $G^h(\mathbf{x}^h)$ be such that

$$G^{h*}(\mathbf{x}^h) \in S^h(R, P^{h*}), G^h(\mathbf{x}^h) \in S^h(R, P^h) \quad (5.11)$$

$$\|G^h - G^{h*}\|_{H_N^{1,h}(\Omega^h)} < \delta. \quad (5.12)$$

Theorem 5.3. Assume that conditions (5.8)-(5.12) hold. Consider the number λ_2 ,

$$\lambda_2 = \lambda_1 (2R, d, M, \Omega^h, B_N, \tau^h, \varepsilon_r^h, h_0) \geq \lambda_1, \quad (5.13)$$

where $\lambda_1 (2R, d, \Omega^h, M^h, B_N, \tau^h, \varepsilon_r^h, h_0)$ is the number in (5.3). Let V_{\min, λ_2}^h be the minimizer of functional (4.46) on the set $\overline{S^h(R, P^h)}$, which was found in Theorem 5.2. Let $\alpha \in (0, R)$ be a number. Suppose that (5.8) is replaced with

$$V^{h*} \in S^h(R - \alpha, P^{h*}), \text{ where } \alpha > C_1\delta. \quad (5.14)$$

Then the vector function V_{\min, λ_2}^h belongs to the open set $S^h(R, P^h)$ and the following accuracy estimate holds:

$$\|V_{\min, \lambda_2}^h - V^{h*}\|_{H_N^{1,h}(\Omega^h)} \leq C_1\delta. \quad (5.15)$$

Consider now the gradient descent method of the minimization of functional (4.46) on the set $\overline{S^h(R, P^h)}$. Let $V_0^h \in B(R/3, P^h)$ be an arbitrary point of this set. We take V_0^h as the starting point of our iterations. Construct the sequence of the gradient descent method as:

$$V_n^h = V_{n-1}^h - \beta (J_{\lambda_2}^h)'(V_{n-1}^h), n = 1, 2, \dots, \quad (5.16)$$

where $\beta > 0$ is a small number. Note that since by Theorem 5.2 functions $(J_{\lambda_2}^h)'(V_{n-1}^h) \in H_{N,0}^{1,h}(\Omega^h)$, then all vector functions V_n^h have the same boundary conditions P^h , see (4.37) and (4.47).

Theorem 5.4. *Let conditions of Theorem 5.3 hold, except that (5.14) is replaced with*

$$V^{h*} \in S^h((R - \alpha)/3, P^{h*}), \text{ where } \alpha/3 > C_1\delta. \quad (5.17)$$

Then there exists a sufficiently small number $\beta > 0$ and a number $\gamma = \gamma(\beta) \in (0, 1)$ such that in (5.16) all functions $V_n^h \in S^h(R, P^h)$ and the following convergence estimates hold

$$\|V_n^h - V_{\min, \lambda_2}^h\|_{H_N^{1,h}(\Omega^h)} \leq \beta^n \|V_0^h - V_{\min, \lambda_2}^h\|_{H_N^{1,h}(\Omega^h)}, \quad (5.18)$$

$$\|V_n^h - V^{h*}\|_{H_N^{1,h}(\Omega^h)} \leq C_1\delta + \beta^n \|V_0^h - V_{\min, \lambda_2}^h\|_{H_N^{1,h}(\Omega^h)}, \quad (5.19)$$

$$\|a_n^h - a^{h*}\|_{L_N^{2,h}(\Omega^h)} \leq C_1\delta + \beta^n \|V_0^h - V_{\min, \lambda_2}^h\|_{H_N^{1,h}(\Omega^h)}, \quad (5.20)$$

where $a_n^h(\mathbf{x}^h)$ and $a_n^{h*}(\mathbf{x}^h)$ are functions which are obtained from V_n^h and V^{h*} respectively via (4.43).

Remarks 5.2:

1. By Definition 1.1 estimates (5.17)-(5.20) imply that the gradient descent method (5.16) of the minimization of the functional $J_{\lambda_2}^h(V^h)$ converges globally for $\lambda = \lambda_2$. Indeed, its starting point V_0^h is an arbitrary point of the set $S(R/3, P^h)$, and $R > 0$ is an arbitrary number.

2. In Theorems 5.3 and 5.4, we fix $\lambda = \lambda_2$ only for the sake of the definiteness. In fact, obvious analogs of these theorems are valid for any $\lambda \geq \lambda_2$.
3. Even though above Theorems 5.2-5.4 require sufficiently large values of the parameter λ , we have numerically established in our computations in section 7 that actually $\lambda = 5$ is sufficient. A similar observation has been consistently made in all above cited works about the convexification method. Conceptually, this is similar with the well known fact from almost any asymptotic theory. Indeed, such a theory typically claims that if a certain parameter X is sufficiently large/small, then a certain formula Y is valid with a good accuracy. However, for any specific numerical implementation with its specific range of parameters only numerical studies can establish which exactly value of X is sufficient to obtain a good accuracy of Y .

6 Proofs

6.1 Proof of Theorem 5.1

Denote

$$L(V^h) = B_N V_z^h + A_1^h V_x^h + A_2^h V_y^h \quad (6.1)$$

and consider $(L(V^h))^2 e^{2\lambda z}$. Since the matrix B_N is invertible, then it follows from (4.39) and (4.45) that

$$\begin{aligned} & \| (A_1^h V_x^h + A_2^h V_y^h) e^{\lambda z} \|_{L^{2,h}(\Omega^h)}^2 \leq C_1 \| V^h e^{\lambda z} \|_{L^{2,h}(\Omega^h)}^2 = \\ & = C_1 \| B_N^{-1} B_N V^h e^{\lambda z} \|_{L^{2,h}(\Omega^h)}^2 \leq C_1 \| (B_N V^h) e^{\lambda z} \|_{L^{2,h}(\Omega^h)}^2, \forall h \geq h_0. \end{aligned}$$

Hence, (6.1) and Cauchy-Schwarz inequality imply

$$\begin{aligned} & \| L(V^h) e^{2\lambda z} \|_{L^{2,h}(\Omega^h)}^2 \geq \\ & \geq \frac{1}{2} \| (B_N V_z^h) e^{\lambda z} \|_{L^{2,h}(\Omega^h)}^2 - C_1 \| (B_N V^h) e^{\lambda z} \|_{L^{2,h}(\Omega^h)}^2. \end{aligned} \quad (6.2)$$

To estimate from the below the first term in the right hand side of (6.2), change variables in it as $W^h = V^h e^{\lambda z}$. Then $V^h = W^h e^{-\lambda z}$. Hence, $V_z^h = (W_z^h - \lambda W^h) e^{-\lambda z}$. Hence, by (4.31) and (4.32)

$$\begin{aligned} & \frac{1}{2} \| (B_N V_z^h) e^{\lambda z} \|_{L^{2,h}(\Omega^h)}^2 = \frac{1}{2} \| (B_N W_z^h) \|_{L^{2,h}(\Omega^h)}^2 \\ & \quad + \frac{\lambda^2}{2} \| (B_N W^h) \|_{L^{2,h}(\Omega^h)}^2 \quad (6.3) \\ & + \sum_{n=0}^{N-1} \sum_{(i,j)=(1,1)}^{(i,j)=(m-1,m-1)} \int_a^b [-\lambda (B_N W_{zn}^h(x_i, y_j, z)) (B_N W_n^h(x_i, y_j, z))] dz. \end{aligned}$$

Next, since $V^h \in H_{N,0}^{1,h}(\Omega^h)$, then $W^h \in H_{N,0}^{1,h}(\Omega^h)$ as well. Hence, by (4.37)

$$\begin{aligned} & \int_a^b [-\lambda (B_N W_{zn}^h(x_i, y_j, z)) (B_N W_n^h(x_i, y_j, z))] dz \\ &= \int_a^b \frac{\partial}{\partial z} \left(\frac{-\lambda}{2} (B_N W_n^h(x_i, y_j, z))^2 \right) dz = 0. \end{aligned} \quad (6.4)$$

Hence, returning from W^h to V^h by $V^h = W^h e^{-\lambda z}$ and using (6.3) and (6.4), we obtain

$$\frac{1}{2} \|(B_N V_z^h) e^{\lambda z}\|_{L^{2,h}(\Omega^h)}^2 \geq \frac{\lambda^2}{2} \|(B_N V^h) e^{\lambda z}\|_{L^{2,h}(\Omega^h)}^2. \quad (6.5)$$

Adding to both sides of (6.5) the term $\|(B_N V_z^h) e^{\lambda z}\|_{L^{2,h}(\Omega^h)}^2 / 2$, we obtain

$$\begin{aligned} & \frac{1}{2} \|(B_N V_z^h) e^{\lambda z}\|_{L^{2,h}(\Omega^h)}^2 \geq \\ & \geq \frac{1}{4} \|(B_N V_z^h) e^{\lambda z}\|_{L^{2,h}(\Omega^h)}^2 + \frac{\lambda^2}{4} \|(B_N V^h) e^{\lambda z}\|_{L^{2,h}(\Omega^h)}^2. \end{aligned} \quad (6.6)$$

Choose $\lambda_0 > 1$ so large that $\lambda_0^2/8 \geq C_1$. Then (6.2) and (6.6) imply the target estimate (5.1). \square

6.2 Proof of Theorem 5.2

Consider two arbitrary points $V_1^h, V_2^h \in \overline{S^h(R, P^h)}$. Let

$$W^h = V_2^h - V_1^h. \quad (6.7)$$

Then by (4.37), (4.47) and the triangle inequality

$$W^h \in S_0^h(2R) = \left\{ V^h \in H_{N,0}^{1,h}(\Omega^h) : \|V^h\|_{H_N^{1,h}(\Omega^h)} \leq 2R \right\}. \quad (6.8)$$

Consider the vector function $F^h(V^h(\mathbf{x}^h), \mathbf{x}^h)$ in (4.41). It follows from (4.20), Remark 5.1 and the multidimensional analog of the Taylor formula [63] that the following representation is valid

$$\begin{aligned} & F(V_2^h(\mathbf{x}^h), \mathbf{x}^h) = F(V_1^h(\mathbf{x}^h) + W^h(\mathbf{x}^h), \mathbf{x}^h) \\ &= F(V_1^h(\mathbf{x}^h), \mathbf{x}^h) + \tilde{F}_1(V_1^h(\mathbf{x}^h), \mathbf{x}^h) W^h(\mathbf{x}^h) \\ & \quad + \tilde{F}_2(V_1^h(\mathbf{x}^h), V_1^h(\mathbf{x}^h) + W^h(\mathbf{x}^h), \mathbf{x}^h), \end{aligned} \quad (6.9)$$

where \tilde{F}_1, \tilde{F}_2 are such that

$$\left| \tilde{F}_1 (V_1^h (\mathbf{x}^h), \mathbf{x}^h) \right| \leq C_1, \quad (6.10)$$

$$\left| \tilde{F}_2 (V_1^h (\mathbf{x}^h), V_1^h (\mathbf{x}^h) + W^h (\mathbf{x}^h), \mathbf{x}^h) \right| \leq C_1 (W^h (\mathbf{x}^h))^2. \quad (6.11)$$

In particular, (6.9) implies that the expression $\tilde{F}_1 (V_1^h (\mathbf{x}^h), \mathbf{x}^h) W^h (\mathbf{x}^h)$ is linear with respect to $W^h (\mathbf{x}^h)$. By (6.1), (6.9) and (6.11)

$$\left\{ \begin{aligned} & [L (V_1^h + W^h) + F (V_1^h (\mathbf{x}^h) + W^h (\mathbf{x}^h), \mathbf{x}^h)]^2 = \\ & = \left[\begin{aligned} & (L (V_1^h) + F (V_1^h (\mathbf{x}^h), \mathbf{x}^h)) + \\ & + (L (W^h) + \tilde{F}_1 (V_1^h (\mathbf{x}^h), \mathbf{x}^h) W^h (\mathbf{x}^h)) + \\ & + \tilde{F}_2 (V_1^h (\mathbf{x}^h), V_1^h (\mathbf{x}^h) + W^h (\mathbf{x}^h), \mathbf{x}^h) \end{aligned} \right]^2 \\ & = [L (V_1^h) + F (V_1^h (\mathbf{x}^h), \mathbf{x}^h)]^2 + \\ & \quad + 2 [L (V_1^h) + F (V_1^h (\mathbf{x}^h), \mathbf{x}^h)] \times \\ & \quad \times [L (W^h) + \tilde{F}_1 (V_1^h (\mathbf{x}^h), \mathbf{x}^h) W^h (\mathbf{x}^h)] + \\ & \quad + 2 [L (V_1^h) + F (V_1^h (\mathbf{x}^h), \mathbf{x}^h)] \times \\ & \quad \times [\tilde{F}_2 (V_1^h (\mathbf{x}^h), V_1^h (\mathbf{x}^h) + W^h (\mathbf{x}^h), \mathbf{x}^h)] + \\ & \quad + \left[\begin{aligned} & L (W^h) + \tilde{F}_1 (V_1^h (\mathbf{x}^h), \mathbf{x}^h) W^h (\mathbf{x}^h) \\ & + \tilde{F}_2 (V_1^h (\mathbf{x}^h), V_1^h (\mathbf{x}^h) + W^h (\mathbf{x}^h), \mathbf{x}^h) \end{aligned} \right]^2. \end{aligned} \right. \quad (6.12)$$

Denote

$$\begin{aligned} I_{\text{lin}} (V_1^h, W^h, \mathbf{x}^h) &= 2 [L (V_1^h) + F (V_1^h (\mathbf{x}^h), \mathbf{x}^h)] \times \\ & \quad \times [L (W^h) + \tilde{F}_1 (V_1^h (\mathbf{x}^h), \mathbf{x}^h) W^h (\mathbf{x}^h)], \end{aligned} \quad (6.13)$$

$$\begin{aligned} I_{\text{nonlin}}^{(1)} (V_1^h, W^h, \mathbf{x}^h) &= 2 [L (V_1^h) + F (V_1^h (\mathbf{x}^h), \mathbf{x}^h)] \times \\ & \quad \times [\tilde{F}_2 (V_1^h (\mathbf{x}^h), V_1^h (\mathbf{x}^h) + W^h (\mathbf{x}^h), \mathbf{x}^h)], \end{aligned} \quad (6.14)$$

$$I_{\text{nonlin}}^{(2)} (V_1^h, W^h, \mathbf{x}^h) = \left[\begin{aligned} & L (W^h) + \tilde{F}_1 (V_1^h (\mathbf{x}^h), \mathbf{x}^h) W^h (\mathbf{x}^h) \\ & + \tilde{F}_2 (V_1^h (\mathbf{x}^h), V_1^h (\mathbf{x}^h) + W^h (\mathbf{x}^h), \mathbf{x}^h) \end{aligned} \right]^2. \quad (6.15)$$

By (6.7) and (6.12)-(6.15)

$$\begin{aligned} & [L (V_2^h) + F (V_2^h (\mathbf{x}^h), \mathbf{x}^h)]^2 - [L (V_1^h) + F (V_1^h (\mathbf{x}^h), \mathbf{x}^h)]^2 \\ & = I_{\text{lin}} (V_1^h, W^h, \mathbf{x}^h) + I_{\text{nonlin}}^{(1)} (V_1^h, W^h, \mathbf{x}^h) + I_{\text{nonlin}}^{(2)} (V_1^h, W^h, \mathbf{x}^h). \end{aligned} \quad (6.16)$$

It follows from (6.1), (6.11), (6.14) and (6.15) that

$$\left\{ \begin{array}{l} \left| I_{\text{nonlin}}^{(1)}(V_1^h, W^h, \mathbf{x}^h) \right| \leq C_1 (W^h(\mathbf{x}^h))^2, \\ \left| I_{\text{nonlin}}^{(2)}(V_1^h, W^h, \mathbf{x}^h) \right| \leq C_1 \left[(W_z^h(\mathbf{x}^h))^2 + (W^h(\mathbf{x}^h))^2 \right], \\ \forall W^h \in S_0^h(2R), \end{array} \right. \quad (6.17)$$

where $S_0^h(2R)$ is defined in (6.8). By (4.46), (6.1), (6.7) and (6.16)

$$\begin{aligned} J_\lambda^h(V_2^h) - J_\lambda^h(V_1^h) &= J_\lambda^h(V_1^h + W^h) - J_\lambda^h(V_1^h) = \quad (6.18) \\ &= \sum_{n=0}^{N-1} \sum_{(i,j)=(1,1)}^{(m-1,m-1)} \int_a^b I_{\text{lin}}(V_1^h(x_i, y_j, z), W^h(x_i, y_j, z), x_i, y_j, z) e^{2\lambda z} dz \\ &+ \sum_{n=0}^{N-1} \sum_{(i,j)=(1,1)}^{(m-1,m-1)} \int_a^b \sum_{k=1}^2 I_{\text{nonlin}}^{(k)}(V_1^h(x_i, y_j, z), W^h(x_i, y_j, z), x_i, y_j, z) e^{2\lambda z} dz. \end{aligned}$$

Using (4.38), (6.17) and (6.18), we obtain

$$\left| \sum_{n=0}^{N-1} \sum_{(i,j)=(1,1)}^{(m-1,m-1)} \int_a^b \sum_{k=1}^2 I_{\text{nonlin}}^{(k)}(V_1^h(x_i, y_j, z), W^h(x_i, y_j, z), x_i, y_j, z) e^{2\lambda z} dz \right| \leq C_1 e^{2\lambda b} \|W^h\|_{H_N^{1,h}(\Omega^h)}^2, \quad \forall W^h \in S_0^h(2R). \quad (6.19)$$

It is clear from (6.13)-(6.15) that the expression in the second line of (6.18) is linear with respect to W^h . On the other hand, the expression in the third line of (6.18) is nonlinear with respect to W^h .

Consider the linear functional $J_{\lambda, \text{lin}}^h(V_1^h)(W^h) : H_{N,0}^{1,h}(\Omega^h) \rightarrow \mathbb{R}$, which is the expression in the second line of (6.18). It follows from (4.36)-(4.39), (6.1), (6.10), (6.13) and (6.18) that

$$|J_{\lambda, \text{lin}}^h(V_1^h)(W^h)| \leq C_1 e^{2\lambda b} \|W^h\|_{H_N^{1,h}(\Omega^h)}, \quad \forall W^h \in H_N^{1,h}(\Omega^h).$$

Hence, $J_{\lambda, \text{lin}}^h(V_1^h)(W^h) : H_{N,0}^{1,h}(\Omega^h) \rightarrow \mathbb{R}$ is a bounded linear functional. By Riesz theorem there exists a vector function $\tilde{J}_{\lambda, \text{lin}}^h(V_1^h) \in H_{N,0}^{1,h}(\Omega^h)$ such that

$$\left(\tilde{J}_{\lambda, \text{lin}}^h(V_1^h), Y^h \right) = J_{\lambda, \text{lin}}^h(V_1^h)(Y^h), \quad \forall Y^h \in H_{N,0}^{1,h}(\Omega^h). \quad (6.20)$$

Also, using (6.17)-(6.20), we obtain

$$\lim_{\|W^h\|_{H_N^{1,h}(\Omega^h)} \rightarrow 0} \frac{J_\lambda^h(V_1^h + W^h) - J_\lambda^h(V_1^h) - J_{\lambda, \text{lin}}^h(V_1^h)(W^h)}{\|W^h\|_{H_N^{1,h}(\Omega^h)}} = 0. \quad (6.21)$$

Hence, $J_{\lambda, \text{lin}}^h(V_1^h) : H_{N,0}^{1,h}(\Omega^h) \rightarrow \mathbb{R}$ is the Fréchet derivative of the functional $J_{\lambda}^h(V^h)$ at the point V_1^h . We denote it as

$$(J_{\lambda}^h)'(V_1^h) := J_{\lambda, \text{lin}}^h(V_1^h). \quad (6.22)$$

The proof of the Lipschitz continuity property (5.2) of $(J_{\lambda}^h)'(V^h)$ is omitted here since it is completely similar with the proof of Theorem 3.1 of [2].

Using (6.10), (6.11), (6.15) and Cauchy-Schwarz inequality, we estimate now $I_{\text{nonlin}}^{(2)}(V_1^h, W^h, \mathbf{x}^h)$ from the below,

$$\begin{aligned} I_{\text{nonlin}}^{(2)}(V_1^h, W^h, \mathbf{x}^h) &\geq \frac{1}{2} (L(W^h))^2 - \\ &- \left[\tilde{F}_1(V_1^h(\mathbf{x}^h), \mathbf{x}^h) W^h(\mathbf{x}^h) + \tilde{F}_2(V_1^h(\mathbf{x}^h), V_1^h(\mathbf{x}^h) + W^h(\mathbf{x}^h), \mathbf{x}^h) \right]^2 \geq \\ &\geq \frac{1}{2} (L(W^h))^2 - C_1 (W^h(\mathbf{x}^h))^2. \end{aligned} \quad (6.23)$$

Thus, Theorem 5.1, (6.18) and (6.22)-(6.23) imply

$$\begin{aligned} &J_{\lambda}^h(V_1^h + W^h) - J_{\lambda}^h(V_1^h) - (J_{\lambda}^h)'(V_1^h)(W^h) \geq \\ &\geq \frac{1}{2} \|L(W^h) e^{\lambda z}\|_{L^{2,h}(\Omega^h)}^2 - C_1 \|W^h e^{\lambda z}\|_{L^{2,h}(\Omega^h)}^2 \geq \\ &\geq \frac{1}{4} \|(B_N W_z^h) e^{\lambda z}\|_{L_N^{2,h}(\Omega^h)}^2 + \frac{\lambda^2}{8} \|(B_N W^h) e^{\lambda z}\|_{L_N^{2,h}(\Omega^h)}^2 - \\ &\quad - C_1 \|W^h e^{\lambda z}\|_{L^{2,h}(\Omega^h)}^2. \end{aligned} \quad (6.24)$$

By Lemma 5.1 there exists a number $\tilde{C}_1 = \tilde{C}_1(B_N, N) > 0$ such that

$$\|(B_N W^h) e^{\lambda z}\|_{L_N^{2,h}(\Omega^h)}^2 \geq \tilde{C}_1 \|W^h e^{\lambda z}\|_{L_N^{2,h}(\Omega^h)}^2, \forall W^h \in L^{2,h}(\Omega^h), \forall \lambda > 0$$

and the same for $\|(B_N W_z^h) e^{\lambda z}\|_{L_N^{2,h}(\Omega^h)}^2$. Hence, (6.24) implies for all $\lambda \geq \lambda_0$

$$\begin{aligned} &J_{\lambda}^h(V_1^h + W^h) - J_{\lambda}^h(V_1^h) - (J_{\lambda}^h)'(V_1^h)(W^h) \\ &\geq \tilde{C}_1 \left(\|W_z^h e^{\lambda z}\|_{L_N^{2,h}(\Omega^h)}^2 + \lambda^2 \|W^h e^{\lambda z}\|_{L_N^{2,h}(\Omega^h)}^2 \right) - C_1 \|W^h e^{\lambda z}\|_{L^{2,h}(\Omega^h)}^2, \end{aligned} \quad (6.25)$$

where $\lambda_0 \geq 1$ was chosen in Theorem 5.1. Choose the number $\lambda_1 \geq \lambda_0$ depending on the parameters listed in (5.3) such that $\tilde{C}_1 \lambda_1^2 / 2 \geq C_1$ and keep in mind Remark 5.1. Then (6.25) implies (5.5) and (5.6). Given (5.5) and (5.6), the existence and uniqueness of the minimizer $V_{\min, \lambda}^h \in \overline{S^h(R, P^h)}$ of the functional $J_{\lambda}^h(V^h)$ on the set $\overline{S(R, P^h)}$ for every $\lambda \geq \lambda_1$ as well as inequality (5.7) follow immediately from a combination of Lemma 2.1 and Theorem 2.1 of [2].

□

6.3 Proof of Theorem 5.3

For each vector function $V^h \in S^h(R, P^h)$ as well as for the vector function $V^{h*} \in S^h(R, P^{h*})$ consider the vector functions \tilde{V}^h and \tilde{V}^{h*} defined as:

$$\tilde{V}^h = V^h - G^h, \quad \tilde{V}^{h*} = V^{h*} - G^{h*}. \quad (6.26)$$

By (4.47), (5.8), (5.11), (6.8), (6.26) and the triangle inequality

$$\tilde{V}^h, \tilde{V}^{h*} \in S_0^h(2R). \quad (6.27)$$

Consider the functional $K_\lambda^h : S_0^h(2R) \rightarrow \mathbb{R}$ defined as

$$K_\lambda^h(\tilde{V}^h) = J_\lambda^h(\tilde{V}^h + G^h). \quad (6.28)$$

Then an obvious analog of Theorem 5.2 implies that this functional is strictly convex on the set $\overline{S_0^h(2R)}$ for all $\lambda \geq \lambda_2$, where λ_2 is taken from (5.13), i.e. in (5.3) R is replaced with $2R$. We now fix $\lambda = \lambda_2$ for the sake of definiteness, see item 2 in Remarks 5.2. Hence, by (5.5) the following estimate holds for all $\tilde{V}_1^h, \tilde{V}_2^h \in S_0^h(2R)$:

$$\begin{aligned} K_{\lambda_2}^h(\tilde{V}_2^h) - K_{\lambda_2}^h(\tilde{V}_1^h) - (K_{\lambda_2}^h)'(\tilde{V}_1^h)(\tilde{V}_2^h - \tilde{V}_1^h) &\geq \\ &\geq C_1 \left\| \tilde{V}_2^h - \tilde{V}_1^h \right\|_{H_N^{1,h}(\Omega^h)}^2. \end{aligned} \quad (6.29)$$

Let $\tilde{V}_{\lambda_2, \min}^h \in \overline{S_0^h(2R)}$ be the unique minimizer of the functional $K_{\lambda_2}^h(\tilde{V}^h)$ in (6.28), which is found in that analog of Theorem 5.2. Then by (5.7) and (6.27) $-(K_{\lambda_2}^h)'(\tilde{V}_{\min, \lambda_2}^h)(\tilde{V}^{h*} - \tilde{V}_{\min, \lambda_2}^h) \leq 0$. Hence, substituting in (6.29) $\tilde{V}_{\min, \lambda_2}^h$ instead of \tilde{V}_1^h and \tilde{V}^{h*} instead of \tilde{V}_2^h and noticing that $-K_{\lambda_2}^h(\tilde{V}_{\min, \lambda_2}^h) \leq 0$, we obtain

$$\left\| \tilde{V}_{\min, \lambda_2}^h - \tilde{V}^{h*} \right\|_{H_N^{1,h}(\Omega^h)} \leq C_1 \sqrt{K_{\lambda_2}^h(\tilde{V}^{h*})}. \quad (6.30)$$

By (6.26) and (6.28)

$$\begin{aligned} K_{\lambda_2}^h(\tilde{V}^{h*}) &= J_{\lambda_2}^h(\tilde{V}^{h*} + G^h) = J_{\lambda_2}^h(\tilde{V}^{h*} + G^{h*} + (G - G^{h*})) \\ &= J_{\lambda_2}^h(V^{h*} + (G - G^{h*})). \end{aligned} \quad (6.31)$$

By (4.46) and (5.9) $J_{\lambda_2}^h(V^{h*}) = 0$. Hence, it follows from (4.46), (5.9), (5.12), (6.9), (6.11) and (6.31) that $K_{\lambda_2}^h(\tilde{V}^{h*}) = J_{\lambda_2}^h(V^{h*} + (G - G^{h*})) \leq C_1 \delta^2$.

Hence, (6.30) implies: $\|\tilde{V}_{\min, \lambda_2}^h - \tilde{V}^{h*}\|_{H_N^{1,h}(\Omega^h)} \leq C_1 \delta$. Hence,

$$\left\| \left(\tilde{V}_{\min, \lambda_2}^h + G \right) - \left(\tilde{V}^{h*} + G^* \right) + (G^* - G) \right\|_{H_N^{1,h}(\Omega^h)} \leq C_1 \delta. \quad (6.32)$$

Combining (6.32) with (5.12), (6.26) and the triangle inequality, we obtain

$$\|U_{\min, \lambda_2}^h - V^{h*}\|_{H_N^{1,h}(\Omega^h)} \leq C_1 \delta, \text{ where } U_{\min, \lambda_2}^h = \tilde{V}_{\min, \lambda_2}^h + G. \quad (6.33)$$

Hence, by (5.14), (6.33) and the triangle inequality

$$\begin{aligned} \|U_{\min, \lambda_2}^h\|_{H_N^{1,h}(\Omega^h)} &\leq \|V^{h*}\|_{H_N^{1,h}(\Omega^h)} + \|U_{\min, \lambda_2}^h - V^{h*}\|_{H_N^{1,h}(\Omega^h)} \leq \\ &\leq R - \alpha + C_1 \delta < R. \end{aligned}$$

Hence, by (4.47)

$$U_{\min, \lambda_2}^h \in S^h(R, P^h). \quad (6.34)$$

Let V_{\min, λ_2}^h be the minimizer of the functional $J_{\lambda_2}^h(V^h)$ on the set $\overline{S^h(R, P^h)}$. This minimizer was found in Theorem 5.2. Denote $W_{\min, \lambda_2}^h = V_{\min, \lambda_2}^h - G$. Then $W_{\min, \lambda_2}^h \in \overline{S_0^h(2R)}$. Hence, $K_{\lambda_2}^h(\tilde{V}_{\min, \lambda_2}^h) \leq K_{\lambda_2}^h(W_{\min, \lambda_2}^h)$. Hence, by (6.28) and (6.33)

$$J_{\lambda_2}(U_{\min, \lambda_2}^h) \leq J_{\lambda_2}(V_{\min, \lambda_2}^h) = \min_{S^h(R, P^h)} J_{\lambda_2}(V^h). \quad (6.35)$$

It follows from (6.34) and (6.35) that U_{\min, λ_2}^h is another minimizer of the functional $J_{\lambda_2}(V^h)$ on the set $\overline{S^h(R, P^h)}$. However, since the minimizer of $J_{\lambda_2}(V^h)$ on $\overline{S^h(R, P^h)}$ is unique, then $U_{\min, \lambda_2}^h = V_{\min, \lambda_2}^h$. This and the inequality in (6.33) imply the accuracy estimate (5.15). \square

6.4 Proof of Theorem 5.4

Let V_{\min, λ_2}^h be again the minimizer of the functional $J_{\lambda_2}(V^h)$ on the set $\overline{S^h(R, P^h)}$. By (5.15) and (5.17) $V_{\min, \lambda_2}^h \in S^h(R/3, P^h)$. Hence, it follows from Theorem 6 of [42] that there exist a sufficiently small number $\beta > 0$ and a number $\gamma = \gamma(\beta) \in (0, 1)$ such that all terms of the sequence (5.16) $V_n^h \in S^h(R, P^h)$ and convergence estimate (5.18) holds. Next, by (5.15), (5.18) and triangle inequality

$$\begin{aligned} \|V_n^h - V^{h*}\|_{H_N^{1,h}(\Omega^h)} &\leq \|V_{\min, \lambda_2}^h - V^{h*}\|_{H_N^{1,h}(\Omega^h)} + \|V_n^h - V_{\min, \lambda_2}^h\|_{H_N^{1,h}(\Omega^h)} \\ &\leq C_1 \delta + \beta^n \|V_0^h - V_{\min, \lambda_2}^h\|_{H_N^{1,h}(\Omega^h)}, \end{aligned}$$

which proves (5.19). Combining the last line of (4.20) with (4.40), (4.43) and (5.19), we obtain (5.20). \square

7 Numerical Studies

7.1 Data simulation

We have conducted our numerical studies in the 2-D case. Below $\mathbf{x} = (x, y)$ and (2.2) and (2.6) become

$$\begin{aligned}\Omega &= \{\mathbf{x} : x \in (-A, A), y \in (a, b)\}, \quad A = 1/2, \quad a = 1, \quad b = 2, \\ \Gamma_d &= \{\mathbf{x}_\alpha = (\alpha, 0) : \alpha \in [-d, d]\}, \quad d = 1/2.\end{aligned}\tag{7.1}$$

In accordance with the conventional practice in the theory of inverse problems, we obtain the boundary data (2.25) via a computational simulation, i.e. via the numerical solution of the Forward Problem (2.21), (2.22). To obtain this solution of the forward problem by equation (3.8), we consider the partition of the intervals (a, b) and $(-d, d)$ in (7.1) as:

$$\left\{ \begin{array}{l} a = y_0 < y_1 < \dots < y_{m_y} = b, \quad y_{j+1} - y_j = h_y, \\ \quad \quad \quad h_y > 0, \quad j = 0, \dots, m_y - 1, \\ -d = \alpha_0 < \alpha_1 < \dots < \alpha_{m_\alpha} = d, \quad \alpha_{j+1} - \alpha_j = h_\alpha, \\ \quad \quad \quad h_\alpha > 0, \quad j = 0, \dots, m_\alpha - 1, \end{array} \right.\tag{7.2}$$

where $m_y, m_\alpha > 1$ are two integers. Define the discrete subsets $(a, b)_y^{h_y}$ and $(-d, d)_\alpha^{h_\alpha}$ of the intervals (a, b) and $(-d, d)$ as $(a, b)_y^{h_y} = \{y_j\}_{j=0}^{m_y}$ and $(-d, d)_\alpha^{h_\alpha} = \{\alpha_j\}_{j=0}^{m_\alpha}$. The fully discrete subset Ω_{discr}^h of the domain Ω is:

$$\begin{aligned}\Omega_{discr} &= \{-A = x_0 < x_1 < \dots < x_m = A\} \times (a, b)_y^{h_y}, \\ &\quad x_{j+1} - x_j = h, \quad j = 0, \dots, m - 1,\end{aligned}\tag{7.3}$$

see (4.26). Denote the corresponding sets of discrete points

$$\begin{aligned}\mathbf{x}_{discr} &= \{(x_i, y_k) \in \Omega_{discr}^h\}, \\ \alpha_{discr} &= \{(\alpha_i, 0, \dots, 0) : \alpha_i \in (-d, d)_\alpha^{h_\alpha}\}.\end{aligned}\tag{7.4}$$

To compute the numerical solution $u(\mathbf{x}_{discr}, \alpha_{discr})$ of the Forward Problem (2.21), (2.22), we need to perform the numerical integration in the integral equation (3.8). We note that the points in the integrals along the geodesic line $\Gamma(\mathbf{x}, \mathbf{x}_\alpha)$ do not necessary belong to the set Ω_{discr}^h . Hence, we describe now our numerical interpolation. For any point $(x^\Gamma, y^\Gamma) \in \Gamma(\mathbf{x}, \mathbf{x}_\alpha)$, we use the following formula of the numerical interpolation to approximate the value $U(x^\Gamma, y^\Gamma)$ of any function U involved in the numerical computation of the

integral over $\Gamma(\mathbf{x}, \mathbf{x}_\alpha)$:

$$\begin{aligned}
 U(x^\Gamma, y^\Gamma) \approx & \frac{1}{hh_y} [(x_{j+1} - x^\Gamma)(y_{k+1} - y^\Gamma)U(x_j, y_k) \\
 & + (x_{j+1} - x^\Gamma)(y^\Gamma - y_k)U(x_j, y_{k+1}) \\
 & + (x^\Gamma - x_j)(y_{k+1} - y^\Gamma)U(x_{j+1}, y_k) \\
 & + (x^\Gamma - x_j)(y^\Gamma - y_k)U(x_{j+1}, y_{k+1})], \\
 \text{for } (x^\Gamma, y^\Gamma) \in & [x_j, x_{j+1}] \times [y_k, y_{k+1}], \text{ see (7.2), (7.3).}
 \end{aligned} \tag{7.5}$$

As to the kernel $K(\mathbf{x}, \alpha, \beta)$ of the integral operator in (2.21), we work below with the 2D Henyey-Greenstein function [24]:

$$K(\mathbf{x}, \alpha, \beta) = H(\alpha, \beta) = \frac{1}{2d} \left[\frac{1 - g^2}{1 + g^2 - 2g \cos(\alpha - \beta)} \right], \quad g = \frac{1}{2}. \tag{7.6}$$

Here, $g = 1/2$ means an anisotropic scattering, which is half ballistic with $g = 0$ an half isotropic scattering with $g = 1$ [15–17]. We take the same function $f(\mathbf{x})$ as the one in (2.7), (2.8) with $\epsilon = 0.05$.

7.2 Numerical results for the inverse problem

Just as in [46], we set

$$\mu_s(\mathbf{x}) = 5, \quad \mathbf{x} \in \Omega, \quad \mu_s(\mathbf{x}) = 0, \quad \mathbf{x} \in \mathbb{R}^2 \setminus \Omega. \tag{7.7}$$

We use formula (2.18) for the coefficient function $a(\mathbf{x})$, and we take in this formula

$$\mu_a(\mathbf{x}) = \begin{cases} c_a = \text{const.} > 0, & \text{inside the tested inclusion,} \\ 0, & \text{outside the tested inclusion.} \end{cases} \tag{7.8}$$

By (2.18), (7.7) and (7.8)

$$\text{correct inclusion/background contrast} = 1 + c_a/5. \tag{7.9}$$

We also set

$$\begin{aligned}
 & \text{computed inclusion/background contrast} \\
 & = 1 + \max(\text{computed } \mu_a(\mathbf{x})) / 5.
 \end{aligned} \tag{7.10}$$

We consider two functions $\varepsilon_r(\mathbf{x})$ in our numerical studies:

$$\varepsilon_r^{(1)}(\mathbf{x}) = \varepsilon_r^{(1)}(x, y) = \begin{cases} 1 + x^2 \ln(y) & y > 1, \\ 1 & \text{otherwise,} \end{cases} \tag{7.11}$$

$$\varepsilon_r^{(2)}(\mathbf{x}) = \varepsilon_r^{(2)}(x, y) = \begin{cases} 1 + (x - 0.5)^2 \ln(y) & y > 1, \\ 1 & \text{otherwise.} \end{cases} \quad (7.12)$$

Both these functions $\varepsilon_r^{(1)}(x, y)$ and $\varepsilon_r^{(2)}(x, y)$ satisfy conditions (2.11)-(2.13).

Using the fast marching toolbox "Toolbox Fast Marching" [54] in MATLAB, we obtain the geodesic lines, and display examples on Figure 1 and Figure 8 for $\varepsilon_r^{(1)}(\mathbf{x})$ in (7.11) and for $\varepsilon_r^{(2)}(\mathbf{x})$ in (7.12), respectively.

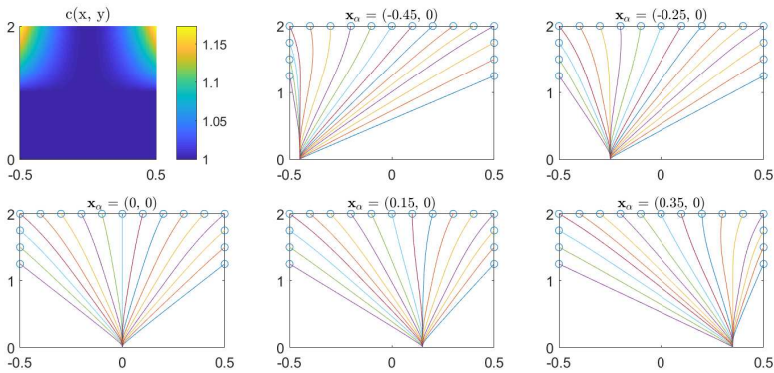


Fig. 1 The geodesic lines with the function $\varepsilon_r(\mathbf{x}) = \varepsilon_r^{(1)}(\mathbf{x})$ given by (7.11) and different positions \mathbf{x}_α of the external source.

The mesh sizes were chosen as $h_x = h_y = h_\alpha = h = 1/20$. Hence, we had total $20 \times 20 \times N$ unknown parameters in our minimization procedure. To solve the minimization problem, we have used the Matlab's built-in function **fminunc** with the quasi-newton algorithm. The iterations of the function **fminunc** were stopped at the iteration number k as soon as

$$|J_\lambda(V_k^h)| < 10^{-2}.$$

The random noise was introduced in the boundary data $g_1(\mathbf{x}, \alpha)$ in (4.13) on the boundary $\partial\Omega$ as:

$$g_1(\mathbf{x}, \alpha) = g_1(\mathbf{x}, \alpha) (1 + \delta \cdot \zeta_{\mathbf{x}}). \quad (7.13)$$

Here $\zeta_{\mathbf{x}}$ is the uniformly distributed random variable in the interval $[0, 1]$ depending on the point $\mathbf{x} \in \partial\Omega$ with $\delta = 0.03$ and $\delta = 0.05$, which correspond respectively to 3% and 5% noise level.

To solve the minimization problem, we need to provide the starting point $V_0^h(\mathbf{x}^h)$ for iterations. In all numerical tests below we choose the starting point as the discrete version of the following vector function $V_0(x, y) =$

$$\begin{aligned} & \left(w_0^{(0)}, \dots, w_{N-1}^{(0)} \right)^T (x, y) : \\ & w_n^{(0)}(x, y) = \frac{1}{2} \left(\frac{(A-x)}{2A} w_n(-A, y) + \frac{(x+A)}{2A} w_n(A, y) \right) \\ & + \frac{1}{2} \left(\frac{(b-y)}{b-a} w_n(x, a) + \frac{(y-a)}{b-a} w_n(x, b) \right), \quad n = 0, \dots, N-1. \end{aligned} \quad (7.14)$$

Expression (7.14) represents the average of linear interpolations of the boundary condition for $w_n(x, y)$ inside of the square Ω with respect to x -direction and y -direction.

There are two parameters we need to choose: N and λ . We find the optimal pair $(N, \lambda) = (5, 3)$ of these parameters in Test 1, see captions for Figures 2 and 3. Interestingly, the same optimal pair was found in [46] for a similar CIP for the regular RTE.

Remark 7.1. *To test the computational performance of the version of the convexification method of this paper, we have chosen letters-like shapes of abnormalities. This is because letters actually have complicated shapes for imaging via solutions of CIPs: they are non convex and have voids.*

Test 1. We test the letter ‘A’ with $c_a = 5$ in (7.8), assuming that the function $\varepsilon_r(\mathbf{x}) = \varepsilon_r^{(1)}(\mathbf{x})$ as in (7.11). We use this test to figure out optimal values of parameters N and λ .

First, we select an appropriate value of N . We use the value of the norms $\|w_n(\mathbf{x})\|_{L_2(\Omega)}$ to indicate the information contained in $w_n(\mathbf{x})$. Corresponding to the forward problem (2.21) and (2.22) for the case when the functions $\mu_s(\mathbf{x})$ and $\mu_a(\mathbf{x})$ are given in (7.7) and (7.8) respectively, and $c_a = 5$ in (7.8), we calculate norms $\|w_n(\mathbf{x})\|_{L_2(\Omega)}$ for $n = 0, \dots, 11$, and display them in Table 1. One can see that the $L_2(\Omega)$ -norm of the function $w_n(\mathbf{x})$ decreases very rapidly when the number n is growing, and these norms, starting from $n = 3$ are much less than those for $n = 0, 1, 2$. More precisely, we have obtained that

$$\frac{\sum_{n=3}^{11} \|w_n(\mathbf{x})\|_{L_2(\Omega)}}{\sum_{n=0}^{11} \|w_n(\mathbf{x})\|_{L_2(\Omega)}} = 0.0039, \quad (7.15)$$

which means less than 1%. We conclude therefore, that we should take in our tests $N = 3$.

Table 1 The $L_2(\Omega)$ -norms of functions $w_n(\mathbf{x})$, $n = 0, 1, \dots, 11$ for the reference Test 1 with $c_a = 5$ in (7.8).

n	0	1	2	3	4	5
$\ w_n(\mathbf{x})\ _{L_2}$	6.5365	1.8766	0.1924	0.0091	0.0071	0.0027
n	6	7	8	9	10	11
$\ w_n(\mathbf{x})\ _{L_2}$	0.0057	0.0020	0.0035	0.0012	0.0017	0.0008

Next, given the value of $N = 3$, we select the optimal value of the parameter λ of the Carleman Weight Function $e^{\lambda z}$ in (4.46). To do this, we test the same letter ‘A’ with $c_a = 5$ inside of it for values of the parameter $\lambda = 0, 1, 2, 3, 4, 5, 6, 8, 20$. Our numerical results are presented on Figure 2. We observe that the images have a low quality for $\lambda = 0, 1$. Then the quality is improved, and it is stabilized at $\lambda = 5$. Thus, we treat $\lambda = 5$ as the optimal value of this parameter.

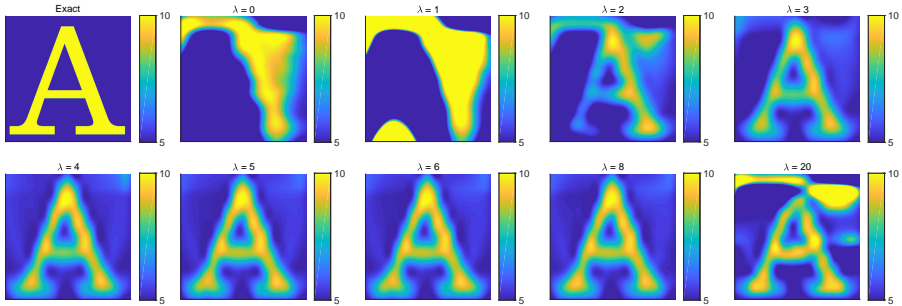


Fig. 2 Test 1. The reconstructed coefficient $a(\mathbf{x})$, where the function $\mu_a(\mathbf{x})$ is given in (7.8) with $c_a = 5$ inside of the letter ‘A’. The function $\varepsilon_r^{(1)}(\mathbf{x})$ is given by (7.11). The goal here is to test different values of the parameter $\lambda = 0, 1, 2, 3, 4, 5, 6, 8, 20$ for $N = 3$. The value of λ can be seen on the top side of each square. The images have a low quality for $\lambda = 0, 1, 2, 3$. Then the quality is improved and is stabilized at $\lambda = 5$. Thus, we select $\lambda = 5$ as an optimal value of this parameter for all follow up tests. On the other hand, the last image is for the case $\lambda = 20$. This image demonstrates that the quality of the reconstructions deteriorates for too large value of λ .

At last, we want to demonstrate numerically again that $N = 3$ is indeed a good choice of N for our optimal value of $\lambda = 5$. Taking $\lambda = 5$, we test the same letter ‘A’ as above with $c_a = 5$ in it, but for $N = 1, 2, 3, 5, 7, 12$. The results are displayed in Figure 3. One can observe that reconstructions have a low quality for $N = 1, 2$. Next, the reconstructions are basically the same for $N = 3, 5, 7, 12$. However, the computational cost increases very rapidly with the increase of N . Thus, we conclude that to balance between the reconstruction accuracy and the computational cost, we should use $N = 3$, which coincides with the above choice.

Test 2. We test the reconstruction of the coefficient $a(\mathbf{x})$ with the shape of the letter ‘A’ where the function $\mu_a(\mathbf{x})$ is given in (7.8). We test different values of the parameter $c_a = 10, 15, 20, 30$ inside of the letter ‘A’. Thus, by (7.9) the inclusion/background contrasts now are respectively $3 : 1, 4 : 1, 5 : 1$ and $6 : 1$. The function $\varepsilon_r(\mathbf{x}) = \varepsilon_r^{(1)}(\mathbf{x})$ as in (7.11). Our computational results for this test are displayed on Figure 4. One can observe that the quality of these images is good for all four cases, although it slightly deteriorates for $c_a = 20$ and $c_a = 30$. The computed inclusion/background contrast is accurate, see (7.10) and compare with (7.9).

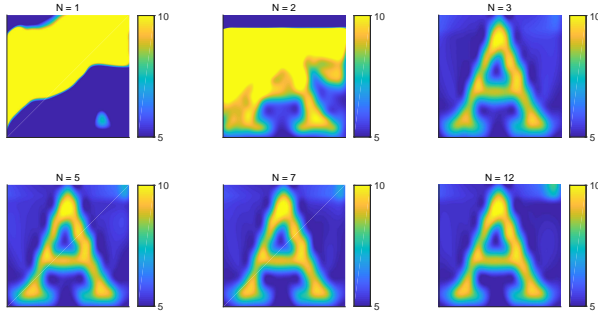


Fig. 3 Test 1. The reconstructed coefficient $a(\mathbf{x})$, where the function $\mu_a(\mathbf{x})$ is given in (7.8) with $c_a = 5$ inside of the letter ‘A’. The function $\varepsilon_r^{(1)}(\mathbf{x})$ is given by (7.11). We took the optimal value of the parameter $\lambda = 5$ (see Figure 2) and have tested different values of the parameter $N = 1, 2, 3, 5, 7, 12$. A low quality can be observed for $N = 1, 2$. The reconstructions are basically the same for $N = 3, 5, 7, 12$. However, the computational cost increases very rapidly with the increase of N . We conclude, therefore, that to balance between the reconstruction accuracy and the computational cost, we should use $N = 3$. Thus, we use below $\lambda = 5$ and $N = 3$.

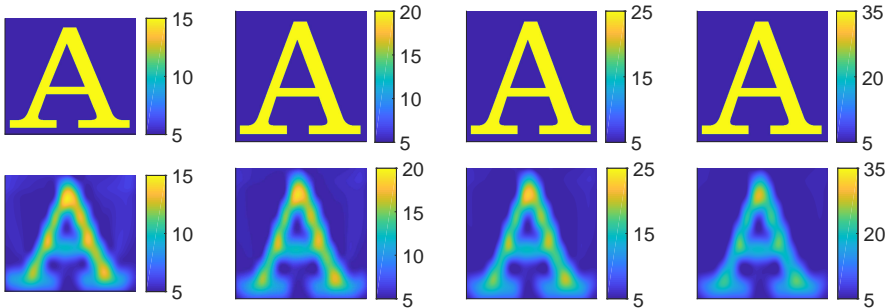


Fig. 4 Test 2. Exact (top) and reconstructed (bottom) coefficient $a(\mathbf{x})$ for $c_a = 10, 15, 20, 30$ inside of the letter ‘A’ as in (7.8) for $N = 3, \lambda = 5$. The function $\varepsilon_r^{(1)}(\mathbf{x})$ is given by (7.11). Thus, by (7.9) the inclusion/background contrasts are respectively 3 : 1, 4 : 1, 5 : 1 and 6 : 1. The image quality remains basically the same for all these values of the parameter c_a , although a slight deterioration of this quality can be observed for $c_a = 20$ and $c_a = 30$. The computed inclusion/background contrasts (7.9) are reconstructed accurately.

Test 3. We test the letter ‘ Ω ’ with $c_a = 5$ in (7.8) and the function $\varepsilon_r(\mathbf{x}) = \varepsilon_r^{(1)}(\mathbf{x})$ as in (7.11), see Figure 5.

Test 4. We test the reconstruction of the coefficient $a(\mathbf{x})$ with the shape of two letters ‘SZ’, where the function $\mu_a(\mathbf{x})$ is given in (7.8) with $c_a = 5$ inside of each of these two letters, and $\mu_a(\mathbf{x}) = 0$ outside of each of these two letters. The function $\varepsilon_r(\mathbf{x}) = \varepsilon_r^{(1)}(\mathbf{x})$ is as in (7.11). SZ are two letters in the name of the city (Shenzhen) were the second and the fifth authors reside.

Test 5. We use noisy data as in (7.13) with $\delta = 0.03$ and $\delta = 0.05$, i.e. with 3% and 5% noise level. We test the reconstruction of the coefficient $a(\mathbf{x})$ with

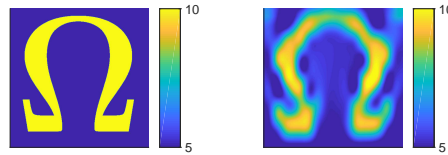


Fig. 5 Test 3. Exact (left) and reconstructed (right) coefficient $a(\mathbf{x})$ for the case when the function $\mu_a(\mathbf{x})$ is given in (7.8) with $c_a = 5$ inside of the letter ‘ Ω ’. The function $\varepsilon_r^{(1)}(\mathbf{x})$ is given by (7.11). Here $N = 3, \lambda = 5$. The reconstruction is accurate, see (7.9) and (7.10).

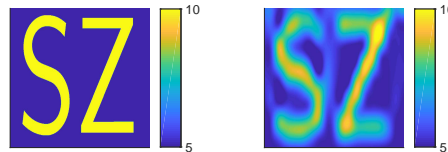


Fig. 6 Test 4. Exact (left) and reconstructed (right) coefficient $a(\mathbf{x})$ for the case when the function $\mu_a(\mathbf{x})$ is given in (7.8) with $c_a = 5$ with the shape of two letters ‘SZ’. In (7.8) $c_a = 5$ inside of each of these two letters and $\mu_a(\mathbf{x}) = 0$ outside of each of these two letters. The function $\varepsilon_r^{(1)}(\mathbf{x})$ is given by (7.11). Here $N = 3, \lambda = 5$. The image quality is lower than one for the case of the single letter Ω on Figure 5. Nevertheless, the quality is still good and the computed inclusion/background contrasts are accurately reconstructed in both letters, see (7.9) and (7.10).

the shape of either the letter ‘A’ or the letter ‘ Ω ’, where the function $\mu_a(\mathbf{x})$ is given in (7.8) with $c_a = 5$ inside of each of these two letters. The function $\varepsilon_r(\mathbf{x}) = \varepsilon_r^{(1)}(\mathbf{x})$ as in (7.11). Here, $N = 3, \lambda = 5$. The results are displayed on Figure 7. One can observe accurate reconstructions in all four cases. In particular, the inclusion/background contrasts are reconstructed accurately, see (7.10) and compare with (7.9).

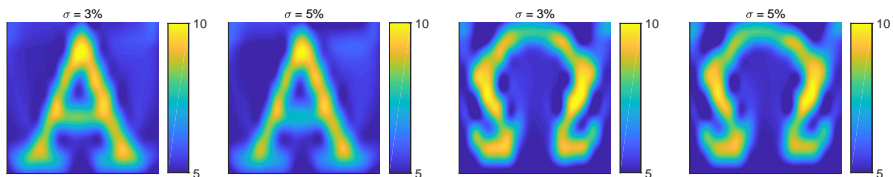


Fig. 7 Test 5. Reconstructed coefficient $a(\mathbf{x})$ with the shape of letters ‘A’ and ‘ Ω ’ with $c_a = 5$ from noise polluted observation data as in (7.13) with $\delta = 0.03$ and $\delta = 0.05$, i.e. with 3% and 5% noise level. The function $\varepsilon_r^{(1)}(\mathbf{x})$ is given by (7.11). Here $N = 3$ and $\lambda = 5$. One can observe accurate reconstructions in all four cases. In particular, the inclusion/background contrasts are reconstructed accurately, see (7.9) and (7.10).

Test 6. We now test the case when $\varepsilon_r(\mathbf{x}) = \varepsilon_r^{(2)}(\mathbf{x})$ is given by (7.12). The geodesic lines for the function $\varepsilon_r(\mathbf{x}) = \varepsilon_r^{(2)}(\mathbf{x})$ in (7.12) are displayed on Figure 8.

We test the reconstruction of the coefficient $a(\mathbf{x})$ with the shape of letters ‘A’, ‘ Ω ’ and ‘SZ’ in Figure 9, Figure 10, and Figure 11, where the function $\mu_a(\mathbf{x})$ is given in (7.8) with $c_a = 5$ inside of each of these letters and $\mu_a(\mathbf{x}) = 0$ outside of these letters.

Similarly with Test 2, we test the reconstruction of the coefficient $a(\mathbf{x})$ with the shape of the letter ‘A’ where the function $\mu_a(\mathbf{x})$ is given in (7.8) with different values of the parameter $c_a = 10, 15, 20, 30$ inside of the letter ‘A’ in Figure 12.

We also use noisy data as in (7.13) with $\delta = 0.03$ and $\delta = 0.05$ to reconstruct the coefficient $a(\mathbf{x})$ with the shape of letters ‘A’ and ‘ Ω ’. The results are exhibited in Figure 13.

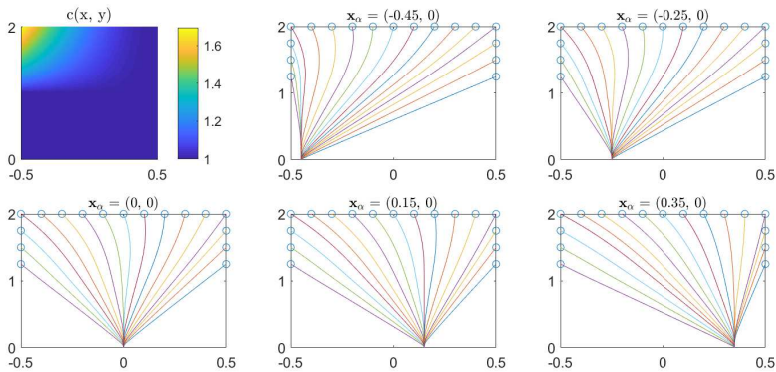


Fig. 8 The geodesic lines with the function $\varepsilon_r^{(2)}(\mathbf{x})$ given by (7.12) and different positions \mathbf{x}_α of the external source.

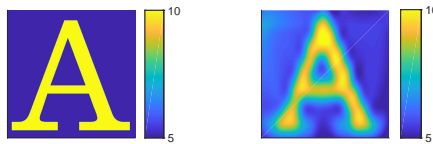


Fig. 9 Test 6. Exact (left) and reconstructed (right) coefficient $a(\mathbf{x})$ for the case when the function $\mu_a(\mathbf{x})$ is given in (7.8) with $c_a = 5$ inside of the letter ‘A’. The function $\varepsilon_r^{(2)}(\mathbf{x})$ is given by (7.12). Here $N = 3, \lambda = 5$. The reconstruction is accurate, see (7.9) and (7.10).

8 Statements and Declarations

Funding: The work of Li was partially supported by the NSF of China No. 11971221, Guangdong NSF Major Fund No. 2021ZDZX1001, the Shenzhen Sci-Tech Fund No. RCJC20200714114556020, JCYJ20200109115422828 and JCYJ20190809150413261.

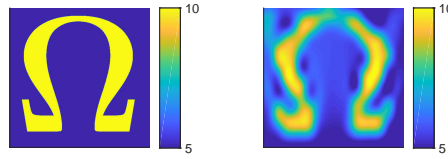


Fig. 10 Test 6. Exact (left) and reconstructed (right) coefficient $a(\mathbf{x})$ for the case when the function $\mu_a(\mathbf{x})$ is given in (7.8) with $c_a = 5$ inside of the letter ‘ Ω ’. The function $\varepsilon_r^{(2)}(\mathbf{x})$ is given by (7.12). Here $N = 3, \lambda = 5$. The reconstruction is accurate, see (7.9) and (7.10).

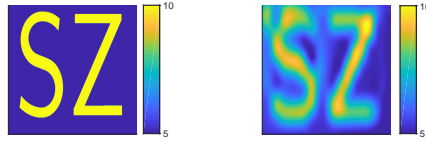


Fig. 11 Test 6. Exact (left) and reconstructed (right) coefficient $a(\mathbf{x})$ for the case when the function $\mu_a(\mathbf{x})$ is given in (7.8) with $c_a = 5$ with the shape of two letters ‘SZ’. In (7.8) $c_a = 5$ inside of each of these two letters and $\mu_a(\mathbf{x}) = 0$ outside of each of these two letters. The function $\varepsilon_r^{(2)}(\mathbf{x})$ is given by (7.12). Here $N = 3, \lambda = 5$. The quality is still good and the computed inclusion/background contrasts are reconstructed accurately in both letters, see (7.9) and (7.10).

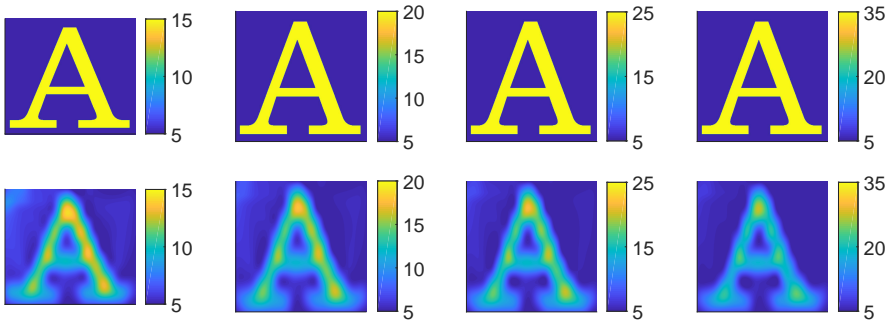


Fig. 12 Test 6. Exact (top) and reconstructed (bottom) coefficient $a(\mathbf{x})$ for $c_a = 10, 15, 20, 30$ inside of the letter ‘A’ as in (7.8) for $N = 3, \lambda = 5$. The function $\varepsilon_r^{(2)}(\mathbf{x})$ is given by (7.12). Thus, by (7.9) the inclusion/background contrasts now are respectively $3 : 1, 4 : 1, 5 : 1$ and $6 : 1$. The image quality remains basically the same for all these values of the parameter c , although some deterioration of this quality can be observed for $c_a = 20$ and $c_a = 30$. The computed inclusion/background contrasts are reconstructed accurately, see (7.9) and (7.10).

The work of L.H. Nguyen was partially supported by National Science Foundation grant DMS-2208159 and by funds provided by the Faculty Research Grant program at University of North Carolina at Charlotte, Fund No. 111272.

The work by V.G. Romanov was performed within the state assignment of the Sobolev Institute of Mathematics of the Siberian Branch of the Russian

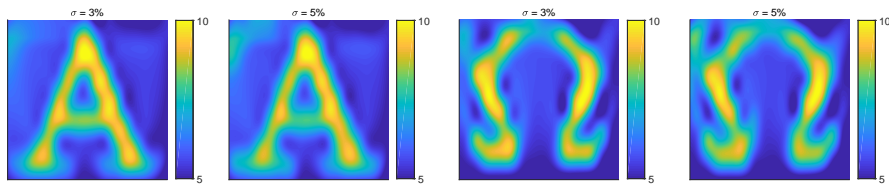


Fig. 13 Test 6. Reconstructed coefficient $a(\mathbf{x})$ with the shape of letters ‘A’ and ‘ Ω ’ with $c_a = 5$ from noise polluted observation data as in (7.13) with $\delta = 0.03$ and $\delta = 0.05$, i.e. with 3% and 5% noise level. The function $c(\mathbf{x})$ is given by (7.12). Here $N = 3$ and $\lambda = 5$. One can observe accurate reconstructions in all four cases. In particular, the inclusion/background contrasts are reconstructed accurately, see (7.9) and (7.10).

Academy of Science, project number FWNF-2022-0009.

Conflicts of interest/Competing interests: The authors have no conflicts of interest to declare that are relevant to the content of this article.

Availability of data and material: The datasets generated during and/or analyzed during the current study are available from the corresponding author on reasonable request.

Code availability: Custom code.

9 Acknowledgments

The work of J. Li was partially supported by the NSF of China grant No. 11971221, Guangdong NSF Major Fund No. 2021ZDZX1001, the Shenzhen Sci-Tech Fund No. RCJC20200714114556020, JCYJ20200109115422828 and JCYJ20190809150413261, National Center for Applied Mathematics Shenzhen, and SUSTech International Center for Mathematics. The work of Nguyen was partially supported by the National Science Foundation grant DMS-2208159 as well as by funds provided by the Faculty Research Grant program at University of North Carolina at Charlotte, Fund No. 111272. The work of V.G. Romanov was performed within the state assignment of the Sobolev Institute of Mathematics of the Siberian Branch of the Russian Academy of Science, project number FWNF-2022-0009.

References

- [1] Asadzadeh, M., Beilina, L.: A stabilized P1 domain decomposition finite element method for time harmonic Maxwell’s equations. *Math. Comput. Simul* **204**, 556-574 (2023)
- [2] Bakushinsky, A.B., Klibanov, M.V., Koshev, N.A.: Carleman weight functions for a globally convergent numerical method for ill-posed Cauchy

- problems for some quasilinear PDEs. *NONLINEAR ANAL-REAL* **34**, 201-224 (2017)
- [3] Bal, G., Tamasan, A.: Inverse source problems in transport equations. *SIAM J. Math. Anal.* **39**, 57-76 (2007)
- [4] Bal, G.: Inverse transport theory and applications. *Inverse Probl.* **25**, 053001 (2009)
- [5] Bal, G., Jollivet, A.: Generalized stability estimates in inverse transport theory. *Inverse Probl. Imaging* **12**, 59-90 (2018)
- [6] Balehowsky, T., Kujanpää, A., Lassas, M., Liimatainen, T.: An inverse problem for the relativistic Boltzmann equation. *Commun. Math. Phys.* **396**, 983-1049 (2022)
- [7] Baudouin, L., De Buhan, M., Ervedoza, S., Osses, A.: Carleman-based reconstruction algorithm for the waves. *SIAM J. Numer. Anal.* **59**, 998-1039 (2021)
- [8] Beilina, L., Lindstrom, E.: An adaptive finite element/finite difference domain decomposition method for applications in microwave imaging. *Electronics* **11**, 1359 (2022)
- [9] Beilina, L., Ruas, V.: On the Maxwell-wave equation coupling problem and its explicit finite-element solution. *Appl. Math.*, online first, DOI: 10.21136/AM.2022.0210-21 (2022)
- [10] Bellassoued, M., Yamamoto, M.: *Carleman Estimates and Applications to Inverse Problems for Hyperbolic Systems*. Springer, Japan (2017)
- [11] Boulakia, M., Buhan, M. de, Schwindt, E.: Numerical reconstruction based on Carleman estimates of a source term in a reaction-diffusion equation. *ESAIM: Control, Optimization and Calculus of Variations* **27**, 1-34 (2021)
- [12] Bukhgeim, A.L., Klibanov, M.V.: Uniqueness in the large of a class of multidimensional inverse problems. *Soviet Mathematics Doklady* **17**, 244-247 (1981)
- [13] Carleman, T.: Sur un problème d'unicité pur les systé émes d'équations aux dériveés partielles ā deux varibales indépendantes. *Ark. Mat. Astr. Fys* **26B**(17), 1-9 (1939)
- [14] Chavent, G.: *Nonlinear Least Squares for Inverse Problems: Theoretical Foundations and Step-by-Step Guide for Applications*. Berlin: Springer Science & Business Media (2010)

- [15] Fujiwara, H., Sadiq, K., Tamasan, A.: A Fourier approach to the inverse source problem in an absorbing and anisotropic scattering medium. *Inverse Probl.* **36**, 015005 (2020)
- [16] Fujiwara, H., Sadiq, K., Tamasan, A.: Numerical reconstruction of radiative sources in an absorbing and nondiffusing scattering medium in two dimensions. *SIAM J. Imag. Sci.* **13**, 535-555 (2020)
- [17] Fujiwara, H., Sadiq, K., Tamasan, A.: A source reconstruction method in two dimensional radiative transport using boundary data measured on an arc. *Inverse Probl.* **37**, 115005 (2021)
- [18] Giorgi, G., Brignone, M., Aramini, R., Piana, M.: Application of the inhomogeneous Lippmann–Schwinger equation to inverse scattering problems. *SIAM J. Appl. Math.* **73**, 212-231 (2013)
- [19] Golgeleyen, F., Yamamoto, M.: Stability for some inverse problems for transport equations. *SIAM J. Math. Anal.* **48**, 2319-2344 (2016)
- [20] Goncharsky, A.V., Romanov, S.Y.: Iterative methods for solving coefficient inverse problems of wave tomography in models with attenuation. *Inverse Probl.* **33**, 025003 (2017)
- [21] Goncharsky, A.V., Romanov, S.Y.: A method of solving the coefficient inverse problems of wave tomography. *Comput. Math. Appl.* **77**, 967-980 (2019)
- [22] Guillement, J., Novikov, R.G.: Inversion of weighted Radon transforms via finite Fourier series weight approximation. *Inverse Probl. Sci. Eng.* **22**, 787-802 (2013)
- [23] Hassi, E., Chorfi, S.-E., Maniar, L.: Stable determination of coefficients in semilinear parabolic system with dynamic boundary conditions. *Inverse Probl.* **38**, 115007 (2022)
- [24] Heino, J., Arridge, S., Sikora, J., Somersalo, E.: Anisotropic effects in highly scattering media. *Phys. Rev. E* **68**, 03198 (2003)
- [25] Hörmander, L.: *Linear Partial Differential Operators*. Springer, Berlin (1963)
- [26] Isakov, V.: Carleman estimates and applications to inverse problems. *Milan J. Math.* **72**, 249-271 (2004)
- [27] Isakov, V.: *Inverse Problems for Partial Differential Equations*. Second Edition, Springer, New York, 2006.

- [28] Kabanikhin, S.I., Novikov, N.S., Oseledets, I.V., Shishlenin, M.A.: Fast Toeplitz linear system inversion for solving two-dimensional acoustic inverse problem. *J. Inverse Ill-Posed Probl.* **23**, 687-700 (2015)
- [29] Kabanikhin, S.I., K. K. Sabelfeld, Novikov, N.S., Shishlenin, M.A.: Numerical solution of an inverse problem of coefficient recovering for a wave equation by a stochastic projection methods. *Monte Carlo Methods Appl.* **21**, 189-203 (2015)
- [30] Khoa, V.A., Klivanov, M.V., Nguyen, L.H.: Convexification for a 3D inverse scattering problem with the moving point source. *SIAM J. Imag. Sci.* **13**, 871-904 (2020)
- [31] Khoa, V.A., Bidney, G.W., Klivanov, M.V., Nguyen, L.H., Sullivan, A., Nguyen, L., Astratov, V.N.: Convexification and experimental data for a 3D inverse scattering problem with the moving point source. *Inverse Probl.* **36**, 085007 (2020)
- [32] Klivanov, M.V.: Inverse problems in the ‘large’ and Carleman bounds. *Differ. Equations* **20**, 755-760 (1984)
- [33] M. V. Klivanov: Inverse problems and Carleman estimates. *Inverse Probl.* **8**, 575-596 (1992)
- [34] Klivanov, M.V., Ioussoupova, O.V.: Uniform strict convexity of a cost functional for three-dimensional inverse scattering problem. *SIAM J. Math. Anal.* **26**, 147-179 (1995)
- [35] Klivanov, M.V.: Global convexity in a three-dimensional inverse acoustic problem. *SIAM J. Math. Anal.* **28**, 1371-1388 (1997)
- [36] Klivanov, M.V., Yamamoto, M.: Exact controllability for the time dependent transport equation. *SIAM J. Control Optim.* **46**, 2071-2195 (2007)
- [37] Klivanov, M.V., Pamyatnykh, S.: Global uniqueness for a coefficient inverse problem for the non-stationary transport equation via Carleman estimate. *J. Math. Anal. Appl.* **343**, 352-365 (2008)
- [38] Klivanov, M.V.: Carleman estimates for global uniqueness, stability and numerical methods for coefficient inverse problems. *J. Inverse Ill-Posed Probl.* **21**, 477-510 (2013)
- [39] Klivanov, M.V.: Convexification of restricted Dirichlet to Neumann map. *J. Inverse Ill-Posed Probl.* **25**, 669-685 (2017)
- [40] Klivanov, M.V., Kolesov, A.E, Nguyen, D.-L.: Convexification method for an inverse scattering problem and its performance for experimental

- backscatter data for buried targets. *SIAM J. Imag. Sci.* **12**, 576-603 (2019)
- [41] Klibanov, M.V., Li, J., Zhang, W.: Convexification for an inverse parabolic problem. *Inverse Probl.* **36**, 085008 (2020)
- [42] Klibanov, M.V., Khoa, V.A., Smirnov, A.V., Nguyen, L.H., Bidney, G.W., Nguyen, L.H., Sullivan, A.J., Astratov, V.N.: Convexification inversion method for nonlinear SAR imaging with experimentally collected data. *J. Applied and Industrial Mathematics* **15**, 413-436 (2021)
- [43] Klibanov, M.V., Li, J.: *Inverse Problems and Carleman Estimates: Global Uniqueness, Global Convergence and Experimental Data*. De Gruyter (2021)
- [44] Klibanov, M.V., Li, J., Zhang, W.: A globally convergent numerical method for a coefficient inverse problem for a wave-like equation. *SIAM J. Sci. Comput.* **44**, A3341-3365 (2022)
- [45] Klibanov, M.V., Romanov, V.G.: A Hölder stability estimate for a coefficient inverse problem for the wave equation with a point source. *Eurasian J. Math. Comp.* **10**(2), 11-25 (2022)
- [46] Klibanov, M.V., Li, J., Nguyen, L., Yang, Z.: Convexification numerical method for a coefficient inverse problem for the radiative transport equation. accepted in *SIAM J. Imag. Sci.*, 2022, arXiv: 2206.11675 (2022)
- [47] Lai, R.Y., Li, Q.: Parameter reconstruction for general transport equation. *SIAM J. Math. Anal.* **52**, 2734-2758 (2020)
- [48] Lavrentiev, M.M., Romanov, V.G., Shishatskii, S.P.: *Ill-Posed Problems of Mathematical Physics and Analysis*. AMS, Providence, R.I. (1986)
- [49] Li, J., Liu, H., Ma, S.: Determining a random schrödinger operator: both potential and source are random. *Commun. Math. Phys.* **381**, 527-556 (2021)
- [50] Li, J., Liu, H., Rondi, L., Uhlmann G.: Regularized Transformation-Optics Cloaking for the Helmholtz Equation: From Partial Cloak to Full Cloak. *Commun. Math. Phys.* **335**(2), 671-712 (2015)
- [51] McDowall, S. R.: An inverse problem for the transport equation in the presence of a Riemannian metric. *Pac. J. Math.* **216**, 303-326 (2004)
- [52] McDowall, S. R.: Optical tomography on simple Riemannian surfaces. *Commun. Partial Differ. Equations* **30**, 1379-1400 (2005)
- [53] Novikov, R., Santacesaria, M.: Monochromatic reconstruction algorithms for two-dimensional multi-channel inverse problems. *Int. Math. Res. Not.*

2013, 1205-1229 (2012)

- [54] Peyre, G.: Toolbox Fast Marching. MATLAB Central File Exchange (2022)
- [55] Romanov, V.G.: Inverse Problems of Mathematical Physics. VNU Press, Utrecht, The Netherlands (1986)
- [56] Romanov, V.G.: Investigation Methods for Inverse Problems. VSP, Utrecht (2002)
- [57] Romanov, V.G.: Inverse problems for differential equations with memory, Eurasian J. Mathematical and Computer Applications, **2**, 51-80 (2014)
- [58] Scales, J.A., Smith, M.L., Fischer, T.L.: Global optimization methods for multimodal inverse problems. J. Comp. Phys. **103**, 258-268 (1992)
- [59] Smirnov, A.V., Klibanov, M.V., Nguyen, L.H.: On an inverse source problem for the full radiative transfer equation with incomplete data. SIAM J. Sci. Comput. **41**, B929-B952 (2019)
- [60] Stefanov, P., Uhlmann, G.: An inverse source problem in optical molecular imaging. Anal. PDE **1**, 115-126 (2008)
- [61] Tamasan, A.: An inverse boundary value problem in two-dimensional transport. Inverse Probl. **18**, 209-219 (2002)
- [62] Tikhonov, A.N., Goncharsky, A.V., Stepanov, V.V., Yagola, A.G.: Numerical methods for the solution of ill-posed problems. Kluwer, London (1995)
- [63] Vajnberg, M.M.: Variational Method and Method of Monotone Operators in the Theory of Nonlinear Equations. Israel Program for Scientific Translations, Jerusalem-London (1973)
- [64] Yamamoto, M.: Carleman estimates for parabolic equations. Topical Review. Inverse Probl. **25**, 123013 (2009)